

Basin inversion and structural architecture as constraints on fluid flow and Pb–Zn mineralisation in the Paleo–Mesoproterozoic sedimentary sequences of northern Australia

George M. Gibson¹

¹Research School of Earth Sciences, Australian National University, Canberra ACT 2601, Australia

Sally Edwards²

²Geological Survey of Queensland, Department of Natural Resources, Mines and Energy, Brisbane, Queensland 4000, Australia

Correspondence to: George M. Gibson (George.gibson@anu.edu.au)

Abstract

As host to several world-class sediment-hosted Pb–Zn deposits and unknown quantities of conventional and unconventional gas, the variably inverted 1730–1640 Ma Calvert and 1640–1575 Ma Isa superbasins of northern Australia have been the subject of numerous seismic reflection studies with a view to better understanding basin architecture and fluid migration pathways. These studies reveal a structural architecture common to inverted sedimentary basins the world over, including much younger examples known to be prospective for oil and gas in the North Sea and elsewhere, and with which they might be usefully compared. Such comparisons lend themselves to suggestions that the mineral and petroleum systems in Paleo–Mesoproterozoic northern Australia may have spatially, if not temporally overlapped and shared a common tectonic driver, consistent with the observation that basinal sequences hosting Pb–Zn mineralisation in northern Australia are bituminous or abnormally enriched in hydrocarbons. Sediment-hosted Pb–Zn mineralisation coeval with basin inversion first occurred during the 1650–1640 Ma Riversleigh Tectonic Event towards the close of the Calvert Superbasin with further pulses taking place during and subsequent to onset of the 1620–1580 Ma Isa Orogeny and final closure of the Isa Superbasin. Mineralisation is typically hosted by the post-rift or syn-inversion fraction of basin fill, contrary to existing interpretations of Pb–Zn ore genesis where the ore-forming fluids are introduced during the rifting or syn-extensional phase of basin development. Mineralising fluids were instead expelled upwards during times of crustal shortening into structural and/or chemical traps developing in the hangingwalls of inverted normal faults. Inverted normal faults predominantly strike NNW and ENE, giving rise to a complex architecture of compartmentalised sub-basins whose individual uplifted basement blocks and doubly-plunging periclinal folds exerted a strong control not only on the distribution and preservation of potential trap rocks but the direction of fluid flow, culminating in the co-location and trapping of mineralising and hydrocarbon fluids in the same carbonaceous rocks. An important case study is the 1575 Ma Century Pb–Zn deposit where the carbonaceous host rocks served as both a reductant and basin seal during the influx of more oxidised mineralising fluids, forcing the latter to give up their Pb and Zn metal. A transpressive tectonic regime in which basin inversion and mineralisation were paired to folding, uplift and erosion during arc-continent or continent-continent collision, and accompanied by orogen-parallel extensional collapse and strike-slip faulting best accounts for the observed relationships.

1 Introduction

40 Northern Australia and its late Paleoproterozoic–early Mesoproterozoic basinal sequences have long
41 attracted the interest of the minerals and petroleum exploration industries. Besides being the world’s single
42 largest repository of sediment-hosted Pb–Zn mineral deposits (Huston et al., 2006;Southgate et al., 2006),
43 these same mineral-rich sequences hold some of the planet’s oldest oil (Jackson et al., 1986) along with an
44 unknown quantity of conventional and unconventional gas (Carr et al., 2019;Gorton and Troup,
45 2018;McConachie et al., 1993). Unsurprisingly, many mineral deposits and their host rocks are bituminous
46 or contain very high proportions of organic carbon (Andrews, 1998;Broadbent et al., 1998;Hutton and
47 Sweet, 1982;Jarrett et al., 2018;McConachie et al., 1993;McGoldrick et al., 2010), raising the possibility
48 that the petroleum and mineralising systems in northern Australia may have spatially, if not temporally,
49 overlapped and share a common tectonic driver. Such a possibility was first entertained for the ca. 1575 Ma
50 Century Pb–Zn deposit (Fig. 1a) where first hydrocarbons and then a more metalliferous ore-forming fluid
51 are thought to have been sequentially trapped following their expulsion from deeper stratigraphic levels
52 during folding and thrusting accompanying the 1620–1580 Ma Isan Orogeny (Broadbent et al., 1998). In
53 this scenario, basin inversion was not only intimately linked to fluid migration and mineralisation but played
54 a key role in generating the structural architecture that brought the petroleum and mineralising systems
55 together in one place. Seismic reflection images for the Lawn Hill Platform have since shown the Century
56 deposit to be hosted by the syn-inversion fraction of basin fill (Gibson et al., 2017;Gibson et al., 2016) and
57 occur in rocks possessing a structural architecture common to inverted basins the world over, including
58 those currently under exploration for oil and gas in the Irish and North seas and north European continental
59 shelf more generally (Cooper et al., 1984;Hayward and Graham, 1989;Lowell, 1995;Thomas and Coward,
60 1995;Turner and Williams, 2004). Thus, not only does basin inversion appear to have been a prerequisite
61 for ore formation at Century, but the structural architecture cannot have appreciably changed during the
62 transition from a hydrocarbon to mineral system lest the similarities with their more modern European
63 counterparts have been lost during crustal shortening. Such conclusions are difficult to reconcile with most
64 existing models for sediment-hosted Pb–Zn mineralisation in northern Australia where ore formation is
65 interpreted to have been syn-extensional and facilitated by fluid migration along normal faults active at the
66 time of basin formation (Huston et al., 2006;Large et al., 2005;Leach et al., 2010;McGoldrick et al., 2010).
67 Alternative exploration strategies for this and other types of sediment-hosted Pb–Zn mineralisation in
68 northern Australia may therefore be warranted that better reflect the similarities with the petroleum system
69 and target the structures formed during basin inversion. Here, we make use of publically available industry
70 and government deep seismic reflection data to show that inversion-related structures of more than one
71 generation and style are widely developed in the late Paleoproterozoic–early Mesoproterozoic basin
72 sequences of northern Australia (Figs. 1 & 2), reflecting successive episodes of crustal shortening during
73 the course of which the majority of Pb–Zn deposits were emplaced (Gibson et al., 2017).

74 **2 Regional geology and basin-forming events of northern Australia**

75 Northern Australia’s late Paleoproterozoic–early Mesoproterozoic basinal sequences belong to one of three
76 superbasins (Figs. 2 & 3) which, together with the overlying Mesoproterozoic South Nicholson Basin (Fig.
77 1a), preserve a 500 million year history of lithospheric extension interrupted by successive episodes of
78 basin inversion, uplift and erosion (Betts et al., 2016;Gibson et al., 2012;Giles et al., 2002;Jackson et al.,
79 2000;Neumann et al., 2006;Southgate et al., 2000a;Sweet, 2017;Yang et al., 2020). The oldest basin
80 inversion event (Fig. 3) occurred after 1840 Ma and is best expressed by the angular unconformity
81 separating the 6–8 km thick 1790–1740 Ma Leichhardt Superbasin (Fig. 2) from an older underlying ≥ 1870
82 Ma crystalline basement (Kalkadoon-Leichhardt Block; Fig. 2) variably intruded by foliated 1860–1840
83 Ma granites (Blake, 1987;Withnall and Hutton, 2013). Clasts of strongly foliated granite and other basement
84 rocks occur widely in conglomerates at the base of the Leichhardt Superbasin (1790 Ma Bottletree
85 Formation) but otherwise its basin fill is only mildly deformed and mainly comprises weakly

86 metamorphosed (greenschist facies) continental tholeiites and rhyolite interstratified with subordinate but
87 still substantial volumes of fluviatile-shallow marine sedimentary rocks. This same cover-basement
88 relationship is also evident on the Murphy Ridge (Fig. 4) farther north where conglomerates (Westmoreland
89 Conglomerate) and sandstones (Wire Creek Sandstone) at the base of the 1790–1710 Ma Tawallah Group
90 (Fig. 3) in the McArthur Basin (Fig. 1b) similarly rest unconformably on an older deformed basement
91 intruded by 1860–1840 Ma granites (Ahmad and Munson, 2013; Rawlings et al., 2008; Sweet, 1984). As
92 with the Kalkadoon-Leichhardt Block, basement granites on the Murphy Ridge were deformed long before
93 the overlying conglomerate was deposited and likely represent exposed fragments of a much more
94 regionally extensive magmatic belt that is continuous at depth and once lay at or close to the eastern margin
95 of the North Australian Craton (Gibson et al., 2008; Korsch et al., 2012). Granites with calc-alkaline
96 compositions occur widely throughout the Kalkadoon-Leichhardt Block (Bierlein et al., 2011) and may
97 originally have formed part of a continental magmatic arc linked to west-dipping subduction beneath the
98 eastern margin of the craton (Bierlein et al., 2008; Korsch et al., 2012). Alternatively, these granites
99 originated in a backarc setting linked to oceanward retreat of a more distal arc built along either the southern
100 or eastern margin of conjoined North and South Australian cratons (Betts et al., 2016; Betts and Giles,
101 2006; Gibson et al., 2018; Gibson et al., 2012; Giles et al., 2002; Giles et al., 2004). Regardless of which
102 interpretation is correct, by 1790 Ma lithospheric extension and thinning were well underway, and northern
103 Australia was subjected to widespread intracontinental rifting, normal faulting and half-graben formation
104 accompanied at deeper crustal levels by elevated heat flow, low pressure-high temperature metamorphism
105 and bimodal magmatic intrusion (Betts et al., 2006; Gibson et al., 2012; Gibson et al., 2008; Holcombe et al.,
106 1991; O'Dea et al., 1997a; Pearson et al., 1991). Lithospheric extension during this phase of basin formation
107 produced mainly northwest-oriented normal faults and half-graben and continued through until ca. 1740
108 Ma when backarc extension and rifting in the Mount Isa region and neighbouring McArthur Basin (Fig. 1a)
109 temporarily ceased and gave way to an episode of thermal subsidence accompanied by the deposition of
110 shallow marine quartzite and carbonate rocks (Gibson et al., 2012; Jackson et al., 2000; O'Dea et al., 1997b).

111 The Leichhardt Superbasin concluded in a period of renewed tectonic instability variously attributed to
112 onset of a 1730–1710 Ma orogenic event (Blaikie et al., 2017) or a renewal in fault-block rotation and tilting
113 (Gibson et al., 2012; Gibson et al., 2008). Either way, uplift and erosion accompanying this event resulted
114 in the formation of a deeply incised and regionally extensive angular unconformity above which
115 conglomerates and redbeds of the Bigie Formation were deposited (Fig. 3). Their deposition marks the start
116 of the 1730–1640 Ma Calvert Superbasin in the Mount Isa region (Figs. 2 & 3) and corresponds to a
117 resumption in backarc extension, bimodal magmatism and rift-related sedimentation across northern
118 Australia (Gibson et al., 2016; Jackson et al., 2000; Southgate et al., 2000a). Both NW-SE and NE-SW
119 extensional directions have been proposed for the Calvert Superbasin (Fig. 3) and questions remain about
120 the primary orientation of half-graben hosting the bulk of basin fill. In the McArthur Basin, this includes
121 basaltic rocks of the 1730–1720 Ma Peters Creek Volcanics and Top Rocky Rhyolite (Page et al.,
122 2000; Rawlings et al., 2008) whereas farther afield on the Lawn Hill Platform (Fig. 1a), the Calvert
123 Superbasin hosts basalts of the 1710–1705 Ma Fiery Creek Volcanics (Fig. 3) and fluviatile-shallow marine
124 sediments of the 1700–1690 Ma Surprise Creek Formation (Big and Prize supersequences; Southgate et al.,
125 2000). At about the same time that these rocks were being laid down across the Lawn Hill Platform, water
126 depths began to substantially increase farther east so that by 1690 Ma basaltic magmas were being extruded
127 and/or intruded into a deep marine basin filled with turbidites (Black et al., 1998; Foster and Austin,
128 2008; Gibson et al., 2018; Gibson et al., 2012; Giles et al., 2002; Glikson et al., 1976; Neumann et al.,
129 2009; Rubenach et al., 2008; Scott et al., 2000; Withnall, 1985). Basaltic magmatism continued through to
130 ca. 1655 Ma in the east by which time the Leichhardt Superbasin and lower parts of the Calvert Superbasin
131 west of the Leichhardt River Fault Trough (Fig. 1a) had been intruded by 1680–1670 Ma A-type granites

132 (Sybella Granite)(Neumann et al., 2006) and partially unroofed on top-to-the-northeast extensional shear
133 zones (Gibson et al., 2008).

134 With the conclusion of bimodal magmatism at 1655 Ma, if not earlier at 1670 Ma in the west, the Calvert
135 Superbasin transitioned from backarc basin to passive rifted continental margin (Baker et al., 2010;Gibson
136 et al., 2018;Gibson et al., 2012;Neumann et al., 2009) and began to cool and subside, precipitating a marine
137 transgression during the course of which the North Australian Craton was buried beneath a post-rift
138 sequence (Gun-Loretta supersequences; Fig. 3) of thin-bedded turbidites, carbonaceous shales, black
139 dolomitic siltstones and carbonate rocks that extended westwards as far as the McArthur Basin (McArthur
140 Group; Figs. 1 & 3) and Lawn Hill Platform (Betts et al., 2016;Betts et al., 2006;Gibson et al., 2012;Gibson
141 et al., 2017;Southgate et al., 2013;Withnall and Hutton, 2013). Passive margin conditions persisted until
142 ca. 1650 Ma by which time northern Australia was subjected to crustal shortening and a further episode of
143 basin inversion (Fig. 3) that lasted until at least 1640 Ma (Riversleigh Tectonic Event) and brought
144 sedimentation in the Calvert Superbasin to a close (Gibson et al., 2018;Gibson et al., 2017;Hinman,
145 1995;Withnall and Hutton, 2013).

146 Thereafter, the tectonic environment fundamentally changed and crustal extension resumed in a north-south
147 direction (Fig. 3), giving rise to the 1640–1575 Ma Isa Superbasin (Fig. 2) and deposition of a further 6-8
148 km of turbiditic sandstones, carbonaceous shales, and dolomitic siltstones (River and Term
149 Supersequences) in fault-bounded basins, predominantly oriented ENE-WSW (Bradshaw et al.,
150 2000;Bradshaw et al., 2018;Gibson et al., 2020;Gorton and Troup, 2018). Despite the resumption in crustal
151 extension, basaltic rocks are absent and, save for a few tuff beds and rare 1620 Ma rhyolite sills, there was
152 no corresponding resurgence in felsic magmatism until after crustal shortening had largely concluded at ca.
153 1590-1580 Ma, some 50–60 Ma later (Black and McCulloch, 1990;Gibson et al., 2018;Withnall and Hutton,
154 2013). The absence of any significant magmatism is in stark contrast to the two older superbasins, leading
155 some researchers to conclude that the Isa Superbasin represents a sag basin, albeit one periodically
156 punctuated by crustal extension (Betts et al., 2003;Betts et al., 2006), whereas others have argued for
157 deposition in a foreland setting (McConachie and Dunster, 1996), pull-apart basin (Scott et al., 1998;Scott
158 et al., 2000;Southgate et al., 2000a) or syn-orogenic basin in which extension was on-going and facilitated
159 by orogen-parallel strike-slip faulting and lateral extrusion of continental crust (Gibson et al., 2020;Gibson
160 et al., 2017). This episode of orogenesis concluded at ca. 1590 Ma (Gibson et al., 2020) or possibly as late
161 as 1580 Ma (Pourteau et al., 2018) before being followed by further crustal extension and successive
162 episodes of pluton-enhanced low pressure-high temperature metamorphism at 1560–1540 Ma and
163 1520–1490 Ma (Duncan et al., 2011;Foster and Rubenach, 2006;Rubenach et al., 2008). Granitic rocks
164 associated with this late metamorphism have both A- and S-type compositions and are mainly to be found
165 in the east where they are demonstrably of post-tectonic origin, truncating and cutting across folds and axial
166 plane fabrics produced during the Isan Orogeny (Foster and Austin, 2008;Giles et al., 2006;Page and Sun,
167 1998;Pollard and McNaughton, 1997;Pollard et al., 1998;Withnall and Hutton, 2013).

168 Granite magmatism concluded in the east at ca. 1500–1490 Ma to be followed by further uplift and erosion
169 across the region before the older sequences were successively buried beneath younger cover rocks of the
170 Mesoproterozoic South Nicholson, Cambrian Georgina and Mesozoic Carpentaria basins (Sweet, 2017).
171 Remnants of these three younger basins are still widely preserved across the Lawn Hill Platform, extending
172 westwards across the Queensland border into the Northern Territory (Fig. 1a) where the South Nicholson
173 Basin is thickest and occupies several different depocentres, including the Carrara Sub-basin (Fig. 4) for
174 which a large volume of high quality seismic reflection data has recently become available (eCat:
175 <http://pid.geoscience.gov.au/dataset/ga/69674>). Although originally acquired as part of a larger study on
176 the South Nicholson Basin (Carr et al., 2019), these data also serve as a window on the structural
177 architecture of the older underlying basinal sequences, and it to this that we now turn.

3 Seismic record of Paleo–Mesoproterozoic basin formation and inversion in northern Australia

Survey lines for seismic reflection data acquired across the Lawn Hill Platform and already in the public domain are shown in Figure 5. Most of these are legacy lines dating back to the late 1980s and early 1990s (Burketown Survey, Comalco)(McConachie et al., 1993) and for which reprocessed data became available in 2014 (Armour Energy). Other lines (Fig. 6a & 6b) were acquired by the minerals industry (Teck Resources, 2011) or minerals industry in collaboration with state and federal Governments (Zinifex, Geological Survey of Queensland and Geoscience Australia, 2006), interpretations of which can be found in several publications and Government records (Bradshaw et al., 2018;Bradshaw and Scott, 1999;Gibson et al., 2017;Gibson et al., 2016;Krassay et al., 2000b;Scott et al., 1998;Southgate et al., 2000b). Results and interpretations of the more recent 2017 South Nicholson Basin survey (Fig. 4) were published jointly by Geoscience Australia and the geological surveys of Queensland and the Northern Territory (Carr et al., 2019) although their interpretation of geology beneath the Carrara Sub-basin (Fig. 4) is not exactly the same as the one presented here, in part owing to uncertainties in extrapolating stratigraphy from existing seismic lines into areas of little or no outcrop or exploratory drilling. The nearest exposures of older rocks are to be found in the Carrara Range immediately north of seismic line 17GA–SN1 (Fig. 4) where a few isolated outcrops of ≥ 1850 Ma basement schist (Kositcin and Carson, 2019) are overlain by an equally poorly exposed sequence (Carrara Range Group) of sandstones and highly altered basaltic rocks (Mitchiebo Volcanics) long regarded as correlatives of the 1780-1775 Ma Seigal Volcanics in the southern McArthur Basin (Ahmad and Munson, 2013;Rawlings et al., 2008;Sweet, 1984) and Eastern Creek Volcanics in the Leichhardt Superbasin (Fig. 3). The Carrara Range Group has been extensively intruded by the 1725 Ma Top Rocky Rhyolite (Jackson et al., 2000;Page et al., 2000) and is unconformably overlain by sedimentary rocks of equivalent age to the Isa Superbasin (Ahmad and Munson, 2013;Rawlings et al., 2008;Sweet, 1984).

In a further departure from previously published interpretations of existing seismic data (Gibson et al., 2017), the Calvert and Isa superbasins are both thought here to comprise discrete syn- and post-inversion sedimentary fractions (Fig. 3). These broadly conform with the sedimentary units or supersequences previously identified at the top of each superbasin (Bradshaw et al., 2000;Bradshaw et al., 2018;Domagala et al., 2000;Krassay et al., 2000a;Krassay et al., 2000b;Southgate et al., 2000a) and have an important bearing on basin evolution, and more particularly on the timing and duration of the basin inversion events that brought successive basin cycles to a close. These and other differences with previously published interpretations can be illustrated with a few well-chosen survey lines and there is no need to include interpretations of the full seismic dataset. All lines chosen here are composite and make for two orthogonal but not completely continuous transects across the Lawn Hill Platform, Carrara Range and neighbouring Carrara Sub-basin (Figs. 4 & 5). For an alternative and slightly different interpretation of these and other lines in the dataset, the reader is referred to Bradshaw and Scott (2009), Bradshaw et al. (2018) and Carr et al. (2019).

3.1 North-south seismic transect across Lawn Hill Platform

This composite transect is made up of several segments (Figs. 6a & 6b) oriented at high angles to the dominant ENE trend of the Isa Superbasin (Fig. 5). Collectively, these segments image a variably inverted southward-thickening sedimentary wedge disrupted by north-dipping faults and bounded at its top and bottom by major unconformity surfaces. Limited outcrop across the Lawn Hill Platform and ties to cross lines for which oil well stratigraphic data are available (Figs. 5 & 7) would further suggest that the greater part of this wedge comprises rocks of the Calvert and Isa superbasins (Bradshaw et al., 2000;Bradshaw and Scott, 1999;Gorton and Troup, 2018;Scott et al., 1998;Southgate et al., 2000a) although the former is missing its full complement of sedimentary units, having lost the Gun Supersequence and a significant

223 amount of the underlying syn-rift package to erosion so that the Loretta Supersequence now rests directly
224 on a severely truncated Prize Supersequence (Fig. 6a). The Loretta Supersequence is itself truncated
225 beneath the River Supersequence and thins northward through onlap onto what remains of the underlying
226 Prize Supersequence (Fig. 6a). For this part of the Lawn Hill Platform, as much as 1700m of sedimentary
227 section is estimated to have been removed by erosion from beneath the River Supersequence (Bradshaw et
228 al., 2000), the greater part of which may have been redeposited farther south in the Leichhardt River Fault
229 Trough (Fig. 1a) where there was a commensurate influx of quartz sand at or before 1640 Ma (Southgate
230 et al., 2000b) during the closing stages of the Calvert Superbasin (Gibson et al., 2017). Basin inversion and
231 an increase in tectonic activity during and subsequent to deposition of the Loretta Supersequence have been
232 invoked as the most likely cause of this erosion (Bradshaw et al., 2000;Gibson et al., 2020;Gibson et al.,
233 2017;Scott et al., 1998), consistent with the observation (Fig. 6a) that this unit is bounded top and bottom
234 by angular unconformities and was laid down at a time of profound change as the depositional environment
235 increasingly began to favour siliciclastic over carbonate sedimentation (Southgate et al., 2000b). Basin
236 inversion at this time is further supported by an increase in redeposited carbonate rocks towards the top of
237 this same supersequence (Southgate et al., 2000b) which, in turn, pass upwards into coarse sandstones and
238 conglomerate (Shady Bore Quartzite), marking not only the base of the unconformably overlying River
239 Supersequence but the start of the Isa Superbasin (Gibson et al., 2017). Similar unconformities have been
240 reported in sequences of comparable age from the southern McArthur Basin (Kunzmann et al.,
241 2019;Rawlings et al., 2008), indicating that this phase of basin inversion, uplift and erosion is more widely
242 developed across northern Australia and is not confined to the Lawn Hill Platform. Conversely, even though
243 rocks of equivalent age to the Leichhardt Superbasin occur widely across the McArthur Basin (Tawallah
244 Group; Fig. 3) as well as farther south in the Leichhardt River Fault Trough (Fig. 1a), they are either missing
245 from the seismic sections investigated here (Figs. 6a & 6b) or reduced to a thin layer sandwiched between
246 basement and the overlying younger basins (cf Scott et al., 1998). Seismic reflections below the level of the
247 Prize Supersequence are too poorly resolved to be confident that the rocks in question belong to one or the
248 other of the two superbasins.

249 In marked contrast, all five supersequences of the Isa Superbasin (Fig. 3) are well imaged along Comalco
250 line 91Bn33–91Bn28, attaining a maximum thickness of 5–6 km (Fig. 6a). Basin architecture along this
251 particular line was first described in detail by Bradshaw et al. (2000) and their interpretation is not dissimilar
252 to the one presented here. More specifically, as in Bradshaw et al. (2000), several inverted normal faults
253 are recognised into which both the River and Term supersequences manifestly thicken (Fig. 6a). Normal
254 faults of this age dip northward and even though some disrupt and offset sedimentary units in the underlying
255 Calvert Superbasin (Loretta and Prize supersequences), there is no reason to conclude that any of these
256 structures ever served as growth faults during deposition of the older sedimentary basin. Rather, these north-
257 dipping faults cut across and postdate stratigraphy in the Calvert Superbasin, and first became active during
258 deposition of the Isa Superbasin. They include the ENE-striking Bluewater and Tin Tank faults (Bradshaw
259 et al., 2018; Pursuit Minerals, 2017), both of which dip to the north and were reactivated in the opposite
260 sense during basin inversion (Fig. 6a). The more steeply-dipping Boga Fault (Minerals, 2017) may similarly
261 have been reactivated at this time but does not share the same dip or strike as the other two structures. It
262 intersects the seismic section at nearly 90° and has a northwest strike more in keeping with other faults of
263 Calvert-age across the region (e.g. Riversleigh Fault; Fig. 5). Moreover, unlike the Bluewater and Tin Tank
264 faults, this structure is associated with a footwall shortcut thrust that not only accommodated a significant
265 amount of strain during basin inversion but shares the same geometry as a similar structure developed in
266 the footwall of the equally steeply-dipping Riversleigh Fault farther south (Fig. 6a). Importantly, neither
267 this footwall thrust nor any of the reactivated normal faults have effected displacements large enough so as
268 to completely disrupt stratigraphy. Instead, stratigraphy continues southward into the hangingwall of the
269 Tin Tank Fault (Fig. 6a) where the Calvert and Isa superbasins have been spectacularly deformed into a

270 km-scale, south-verging antiformal fold (Punjaub Structure). The River and Term supersequences attain
271 maximum stratigraphic thickness in the core of this fold which is both strikingly asymmetric in character
272 and by far the most obvious inversion structure developed along this particular segment of the north-south
273 transect (Fig. 6a).

274 Conversely, through a combination of onlap and truncation, the Lawn and Wide supersequences both lose
275 thickness over the crest of this same antiformal fold (Fig. 6a). Despite the loss of sedimentary record, and
276 even more obvious truncation at the base of the overlying Mesozoic cover rocks (Fig. 6a), this thinning
277 appears to be an original depositional feature with neither sedimentary unit ever having maintained constant
278 stratigraphic across the fold. Instead, their sedimentary thickness was strongly influenced by the presence
279 of this structure. It follows that the Punjaub Structure either already existed by the time the Lawn and Wide
280 supersequences were deposited or the fold was actively growing during the course of their deposition.
281 Irrespective of which interpretation is correct, these two units cannot be part of the syn-extensional growth
282 package. Rather, extension in the Isa Superbasin had already come to a close before sedimentation ceased,
283 and both units more rightly belong to the post-rift or syn-inversion fraction of basin fill. A similar
284 conclusion was reached by Gibson et al (2017) for the Lawn and Wide supersequences exposed farther
285 south along seismic line 06GA–M2 in the Century region (see below). Basin architecture in these two
286 regions shares many similarities, not least of which is a folded and locally inverted basin fill which, in the
287 Century region, is known to host a world class Pb–Zn mineral deposit (Southgate et al., 2000a; Southgate
288 et al., 2006). Onlap of the River Supersequence onto older folded units in the cores of the doubly-plunging
289 Mount Caroline and Ploughed Mountain folds (Figs. 1b & 6b) would further suggest that this was not the
290 only episode of basin inversion to have affected the rocks of the Lawn Hill Platform. However, as elsewhere
291 across northern Australia, the existence of the older deformational event has largely gone unrecognised
292 owing to extensive overprinting during the 1620–1580 Ma Isa Orogeny and at least one additional
293 shortening event that postdates the Isa Orogeny and folded all units up to and including the South Nicholson
294 Basin (Fig. 6a). Doubly-plunging periclinal folds like Ploughed Mountain and Mount Caroline (Figs. 1b &
295 6b) may similarly be an expression of this younger event although, as already mentioned, they more likely
296 first came into existence during the earlier basin inversion event and were subsequently reactivated and/or
297 tightened during later deformation.

298 **3.2 West-east seismic transect through the Calvert and Isa superbasins**

299 As with the north-south transect, seismic sections oriented west-east or northeast-southwest are dominated
300 by rocks of the Calvert and Isa superbasins and share the same wedge-like geometry (Fig. 7a & 7b). This
301 wedge-like geometry is particularly well illustrated in composite section 89Bn07–89Bn03–89Bn06 and
302 shows the Isa Superbasin thickening from east to west with the main sedimentary depocentre located
303 towards the southwest as might be expected in a seismic section oriented parallel or subparallel to basin
304 strike. Absent or difficult to recognise in either this section or 90Bn10 (Fig. 7b) are structures that might
305 have unequivocally served as growth faults during development of the Isa Superbasin. Normal faults of this
306 age dip predominantly northward (Fig. 6a) and as such are anticipated to have shallow-dipping or sub-
307 horizontal traces in west-east oriented seismic sections but still cut up-section all the way to the Term
308 Supersequence. Few structures with the requisite shallow dips have been identified in either section, and
309 the only evidence of structural control on basin fill occurs at deeper levels in the Calvert Superbasin where
310 the Loretta and Prize supersequences both thicken into northeast-dipping structures (Fig. 7b). Although
311 locally disrupted by later sub-vertical faults, these structures demonstrably served as growth faults during
312 deposition of the Calvert Superbasin and typically cut up-section no farther than the Loretta Supersequence
313 (Fig. 7b). However, like the Riversleigh Fault (Fig. 8a) and other faults sharing the same northwest trend
314 on the Lawn Hill Platform, these structures were subsequently reactivated in an oblique sense and continued

315 to act as growth faults during deposition of the younger River and lowermost Term supersequences (Fig.
316 8a).

317 Following deposition of the River and lowermost Term supersequences, extension and normal faulting
318 across the Lawn Hill Platform ceased and the syn-rift fraction of basin fill was buried beneath a post-rift
319 blanket of near constant thickness that comprises the rest of the Term Supersequence (Figs. 7a & 7b). This
320 was superseded, in turn, by deposition of the Lawn, Wide and Doom supersequences which, together, make
321 up the syn-inversion package and conspicuously thin over the crest of folds developed in the hangingwalls
322 of inverted normal faults such as the Tin Tank and Riversleigh structures (Figs. 6a & 8a). Thinning of the
323 younger stratigraphic units across the crests of antiformal folds is no less conspicuous in the west-east
324 oriented seismic sections shown here and is particularly evident where the underlying syn-rift sequence
325 attains maximum thickness and has been more undergone the greatest amount of inversion-related uplift
326 (Figs. 7a & 7b). Such relationships are not unexpected and conform to theoretical expectations for inverted
327 sedimentary basins (Cooper et al., 1989). They also lend support to the idea that basin inversion, and
328 deformation more generally, had already commenced across the Lawn Hill Platform before sedimentation
329 in the Isa Superbasin had come to a close (Gibson et al., 2017).

330 Conversely, the few large faults cutting upwards through these younger stratigraphic units from deeper
331 levels in the Isa or Calvert superbasins are too steeply dipping to be reactivated normal faults or inversion-
332 related structures and more likely represent strike-slip faults. Their age is not well constrained although
333 some cut up-section as far as the South Nicholson Basin and evidently formed late. Others terminate at
334 deeper stratigraphic levels and may be more like the Riversleigh Fault (Fig. 8a) which was reactivated in a
335 strike-slip sense during and subsequent to the onset of north-south extension and concomitant deposition
336 of the River and Term supersequences (Gibson et al., 2017).

337 **3.3 Basin inversion west of the Lawn Hill Platform**

338 Seismic reflection data collected west of the Lawn Hill Platform with a view to better understanding the
339 mineral and hydrocarbon potential of the poorly exposed Mesoproterozoic South Nicholson Basin, and
340 Carrara Sub-basin in particular (Fig. 4), have already been interpreted and published in their entirety (Carr
341 et al., 2019), and this paper is only concerned with parts of the dataset that may be used to shed further light
342 on basin architecture in the underlying older sequences. Especially pertinent in this regard are the
343 constraints imposed by the eastern half of seismic line 17GA–SN1 (Fig. 8b) which joins onto the existing
344 Century line (06GA–M2) just west of the Riversleigh Fault (Figs. 5 & 8a). As such, these two lines make
345 for a single continuous and greatly expanded west-east transect through this part of northern Australia and
346 might be expected to share a common older geology and basin architecture (Fig. 8b). An interpretation of
347 these two lines is presented in Figures 8a – 8c and would appear to confirm that this is indeed the case for
348 the younger post-rift and syn-inversion fractions of basin fill in the Isa Superbasin. These two fractions not
349 only continue without break from one seismic line into the other but can be traced westwards beneath the
350 Carrara Sub-basin for 10s of kilometres before eventually thinning over a basement high located just south
351 of the Carrara Range (Fig. 4) where seismic lines 17GA–SN1 and SN2 intersect (see also Carr et al., 2019).
352 This basement high developed in the hangingwall of a major south- or southeast-dipping fault or fault zone
353 (Little Range Fault Zone) but owing to the west-east orientation of the seismic profile (Fig. 4), this structure
354 and its hangingwall sequences are imaged in oblique section and thus dip far less steeply than in other
355 sections oriented at higher angles to fault strike (e.g. 17GA-SN2 and 17GA-SN4). Basement rocks, along
356 with the rest of the hangingwall sequence, have nevertheless been clearly inverted and take the form of a
357 broad arch or subdued fold in the seismic image (Fig. 8b). No less importantly, from the thinning of younger
358 sedimentary units onto the eastern flank of this fold (Fig. 8b), it may be further deduced that basin inversion,
359 as in the Punjaub Structure, was already underway before the last of the Isa Superbasin had been deposited.

360 Thinning of the younger stratigraphic units aside, it is equally evident from the seismic data that the
361 hangingwall of the Little Range Fault Zone comprises a less than complete sedimentary record (Fig. 8b).
362 The syn-rift fraction of basin fill (River and lowermost Term supersequences) and any unit that might be
363 reliably identified as part of the Calvert Superbasin are missing and do not appear to extend any farther
364 west than the Riversleigh Fault (Figs. 8a & 8b). Particularly conspicuous by its absence is the Loretta
365 Supersequence whose transparent to weakly reflective character in seismic sections (Bradshaw et al.,
366 2000;Southgate et al., 2000a) is usually enough to distinguish it from other stratigraphic units in the Calvert
367 and Isa Superbasins (e.g. Figs. 6 –7). Either this and the other missing sedimentary units were never
368 deposited west of the Riversleigh Fault or, as elsewhere across the region, these rocks have been removed
369 by erosion so that younger elements of the Isa Superbasin have come to directly overlie older rocks thought
370 (Gibson et al., 2017) to form part of the Leichhardt Superbasin (Figs. 8a & 8b). Stratigraphy in this older
371 basin is variably truncated beneath rocks of the overlying Isa Superbasin and, like them, can be traced
372 westwards for some distance towards the Little Range Fault Zone and its basement high, and over the top
373 of which the older rocks almost reach the surface (Fig. 8b). Nowhere, however, along the seismic line are
374 the older rocks actually exposed. A thin veneer of Cambrian and/or Mesozoic sediments (Georgina and
375 Carpentaria basins) always intervenes although rocks long thought (Ahmad and Munson, 2013;Rawlings
376 et al., 2008) to be correlatives of the Leichhardt Superbasin (Fig. 3) are exposed north of the seismic line
377 in the Carrara Range (Carrara Range Group: Fig. 4). Moreover, these rocks have since been shown to have
378 the same age as the Leichhardt Superbasin based on strikingly similar detrital zircon populations (Kositcin
379 and Carson, 2019). Moreover, these older rocks rest unconformably on ≥ 1840 Ma psammopelitic schists
380 which not only represent basement to the Carrara Range Group (Ahmad and Munson, 2013;Rawlings et al.,
381 2008) but likely serve as a good proxy for unexposed basement along the seismic line a short distance to
382 the south.

383 West of the Little Range Fault Zone is a second, even larger uplifted basement block or horst bounded on
384 its eastern side by a steeply-dipping fault and inverted sedimentary basin (Fig. 8c) filled almost entirely by
385 rocks of the Isa Superbasin. Basin fill is up to 10 km-thick and strikingly similar in both volume and
386 geometry to the correlative sequence exposed in the hangingwall of the Riversleigh Fault farther east (Fig.
387 8a). As with the latter, this includes the full complement of post-rift and syn-inversion sedimentary units
388 (Lawn, Wide and Doom supersequences) as well as a thicker syn-rift package of more strongly reflective
389 rocks interpreted here (Fig. 8c) to be made up of the River and Term supersequences. The River
390 Supersequence is particularly well represented, thickening into the Old Man's Fault (informal name) and
391 characteristically exhibiting a wedge-like geometry that thins eastwards through overlap onto the adjacent
392 basement high and its cap of Leichhardt Superbasin (Fig. 8c). Its contact with the underlying older rocks
393 just west of the Little Range Fault Zone is an angular unconformity beneath which the Leichhardt
394 Superbasin is abruptly truncated or lost altogether so that the Isa Superbasin rests directly on the underlying
395 basement (Fig. 8c). Significantly, this same angular relationship has been observed in outcrop in the Carrara
396 Range (Sweet, 1984) where rocks of the McNamara Group (Isa Superbasin) directly overlie the Carrara
397 Range Group (Leichhardt Superbasin equivalents). It is thus not unreasonable to conclude that the River
398 Supersequence was deposited on an already uplifted and eroded surface that cuts downward ever more
399 deeply in a southerly or east to west direction so as to expose progressively older elements of the regional
400 stratigraphy in and around the Carrara Range. Moreover, even though the bulk of this uplift and erosion
401 likely occurred during the 1650–1640 Riversleigh Tectonic Event immediately prior to deposition of the
402 River Supersequence, the possibility that some of it dates from an even older 1730 Ma episode of
403 deformation better known from the McArthur Basin as the mid-Tawallah Compressional Event (Ahmad
404 and Munson, 2013) cannot be excluded. Notwithstanding such uncertainties, basement and its bounding
405 faults clearly played an important role in controlling basin architecture and continued to be active long after
406 deposition of the Isa Superbasin had concluded as both the South Nicholson and Georgina basins similarly

407 thin across them (Fig. 8c). Equally notable in this context is an obvious reversal in basin and fault polarity
408 on either side of the larger basement horst block (Fig. 8b).

409 **3.4 North-south seismic sections orthogonal to 17GA-SN1**

410 As a further check on basin geometry and structural architecture to the west of the Lawn Hill Platform, two
411 sections (17GA-SN2 and 17GA-SN4) were selected for interpretation in a direction at a high angle or
412 orthogonal to 17GA-SN1 (Figs. 9a & 9b). With its NW-SE orientation, seismic line 17GA-SN2 cuts across
413 many of the same structures imaged in 17GA-SN1, most notably at least one crustal-scale south- or
414 southeast-dipping shear zone or fault system that extends downward into the lower crust and possibly as
415 far as the MOHO (Figs. 8b & 9a). This shear zone is several hundred metres wide and is likely the same
416 reactivated basement structure identified as the Little Range Fault Zone along line 17GA-SN1; it has
417 variably deformed rocks of the Leichhardt and Isa superbasins in its hangingwall (Fig. 9a) and appears to
418 have served as a thrust system during basin inversion, effecting upward displacement not only of the former
419 but the underlying basement rocks. The most obvious difference between lines 17GA-SN1 and 17GA-SN2
420 is the thick wedge-like basinal sequence imaged down to 7.0 seconds TWT in the hangingwall of this same
421 shear zone (Fig. 9a). This basinal sequence lies below the interpreted base of the Leichhardt Superbasin in
422 line 17GA-SN1 (Fig. 8b) and either represents an entirely separate older volcanic/sedimentary package or
423 a continuation of the Leichhardt Superbasin downward to much greater depths than is immediately apparent
424 in the west-east oriented seismic section. In the absence of independent information, it is not possible to
425 discriminate between these two possibilities except to say that the same package is evidently present in line
426 17GA-SN1 and corresponds to a zone of non-reflective crust which at a depth of 10 kilometres or more
427 seems much too deep for the Leichhardt Superbasin (Fig. 9a) and shares none of the higher amplitude
428 reflectors common to other seismic lines through this basin elsewhere in the Mount Isa region (e.g.
429 06GA-M3; Gibson et al., 2016). Several other low-angle faults imaged in lines 17GA-SN1 and 17GA-SN2
430 also root downward into this zone (Figs. 8b & 9a) although neither they nor the surfaces bounding the older
431 sedimentary package are particularly conspicuous or maintain their individual character at depth. Rather,
432 all of these faults and surfaces merge downward into one seismically bland and homogenised region of
433 middle crust more in keeping with expectations for metamorphic basement than the Leichhardt Superbasin.
434 Moreover, because line 17GA-SN1 is probably more closely aligned with lithological strike in the older
435 sedimentary package and its bounding surfaces, their apparent dip in this particular seismic section is close
436 to zero, resulting in surfaces whose traces are subhorizontal and parallel to each other. Only along line
437 17GA-SN2 is the northern dip of this older seismic package discernible.

438 As with the other two seismic lines across the South Nicholson Basin, 17GA-SN4 has imaged a basement
439 block overlain by a southward-thickening wedge of sedimentary rocks mainly belonging to the Isa
440 Superbasin but beneath which there is a variably truncated and faulted older sequence. This older sequence
441 rests directly on basement and likely incorporates correlatives of the Leichhardt Superbasin (Fig. 9b).
442 Seemingly missing again is the Calvert Superbasin and its place has been taken up by a package of rocks
443 (Fig. 9b) whose seismic character (short, high amplitude reflectors) is a better fit for the River and/or Term
444 Supersequence as opposed to the Loretta or Prize supersequences. Lying above this package are several
445 sedimentary units identified elsewhere in this paper as belonging to the post-rift and syn-inversion fractions
446 of basin fill in the Isa Superbasin. They, in turn, are overlain by younger sediments of the South Nicholson
447 and Georgina basins although the latter is very thin and represents no more than a veneer over the underlying
448 rocks (Fig. 9b).

449 Importantly, essentially the same stratigraphic package can be identified north of the seismically imaged
450 basement block, except that all sedimentary units, including those making up the South Nicholson Basin,
451 are appreciably thicker and have a different geometry, pointing to deposition in a separate sub-basin to the

452 Carrara Sub-basin (Fig. 9b). In keeping with this interpretation, the two depocentres are separated by a
453 major fault which dips steeply south and is likely an along-strike continuation of the same south-dipping
454 fault system (Little Range Fault Zone) imaged farther west along seismic lines 17GA-SN1 and SN2. As
455 with the other two structures, this fault played an equally important role in basin formation and was
456 reactivated on more than one occasion because sedimentary units in its hangingwall, up to and including
457 the South Nicholson Basin, have all been inverted whereas older rocks in its footwall are cut by this
458 basement fault and terminate abruptly against it. This includes rocks of the River and/or Term
459 supersequences which were deposited on an older and already folded older sequence taken here to be
460 Paleoproterozoic Carrara Range Group (Fig. 9b) and thus part of the Leichhardt Superbasin (Fig. 3). No
461 less conspicuously, this older sequence thickens towards basement and its bounding fault, whereas
462 sedimentary sequences making up the overlying South Nicholson Basin and higher levels of the Isa
463 Superbasin (Lawn through to Doom supersequences) do the opposite; they instead thin towards this
464 basement high and likely overlapped the latter at the time these rocks were being deposited. The seismic
465 images are consistent with such an interpretation, particularly for the higher level sedimentary units (Fig.
466 9b), which still show significant amounts of thinning over the adjacent basement high despite successive
467 episode of fault reactivation. Sedimentation, paired to uplift and erosion has been observed before in the
468 Paleo-Mesoproterozoic basins of Northern Australia and usually attributed to repeated episodes of rift-sag
469 (Betts et al., 2016; Betts et al., 2003; Betts et al., 2006; O'Dea et al., 1997b) or strike-slip faulting along basin-
470 bounding structures (Scott et al., 1998; Southgate et al., 2000b). Basin inversion with a few notable
471 exceptions (Blaikie et al., 2017; Broadbent et al., 1998; Gibson et al., 2017) was largely treated as a late or
472 secondary process and thus incidental to the formation of Pb–Zn mineral deposits. Interpreted seismic data
473 presented in this paper would suggest otherwise and that basin inversion as a process had a far greater
474 impact on basin history and mineralisation than has hitherto been recognised.

475 **4 Discussion**

476 **4.1 Basin inversion structures: timing and distribution**

477 Inverted extensional basins and their structural architecture have been widely investigated and described
478 following numerous field studies combined with the results of numerical modelling and sandbox
479 experiments (Cooper et al., 1989; Hayward and Graham, 1989; McClay et al., 2002; McClay and White,
480 1995; Turner and Williams, 2004). Emphasised in most of these studies is the strongly asymmetric nature
481 of the pre-existing basin fill and the consequences of shortening a sedimentary sequence whose individual
482 unit lengths are all different and increase upward from bottom to top of the section (Hayward and Graham,
483 1989; Lowell, 1995; Turner and Williams, 2004). The net result during shortening is development of an
484 equally asymmetric fold in the hangingwall of the original normal fault which may or may not have been
485 reactivated during the process. This hangingwall fold is one of the most distinctive features of basin
486 inversion and may be regarded as a diagnostic feature, particularly in cases where folding is enhanced by
487 the reactivation of coeval antithetic structures leading to the expulsion of basin fill in opposite directions.
488 Further enhancements of the basic inverted structure may occur where the normal fault locks up early and
489 strain is transferred to a footwall shortcut thrust or taken up by some other structure such as a strike-slip
490 fault (Dooley and McClay, 1997; McClay, 1995; McClay et al., 2002). These and other variations on
491 structural architecture developed during basin inversion (Martínez et al., 2012) are illustrated in Figure 10.
492 All examples are from inverted basins of Mesozoic or younger age but are clearly no less relevant in the
493 case of the older basins described here from northern Australia. Footwall shortcut thrusts have been
494 captured in several of the seismic sections but are conspicuously well developed in the footwalls of the
495 Riversleigh (06GA–M2) and Boga structures (Figs. 8a & 6b). However, by far the most common and
496 widely imaged structure is the hangingwall antiform (Fig. 10). Moreover, this same structural feature is
497 evident in all sections irrespective of whether they are oriented north-south or west-east, supporting

498 suggestions made elsewhere that there has been more than one episode of basin inversion and that these
499 were imposed on basins that were originally orthogonal to one another. As such, basin inversion affords
500 clues to basin orientation before and after successive episodes of crustal shortening got underway and it is
501 to this topic that we now turn.

502 The Isa Superbasin is best known from the Lawn Hill Platform (Fig. 5) and has been previously interpreted
503 as a sag or foreland basin deformed during a subsequent north-south shortening event identified as the Isan
504 Orogeny (Betts et al., 2003;McConachie et al., 1993;McConachie and Dunster, 1996). More recently, an
505 extensional origin has been proposed for this same basin consistent with seismic data and general thickening
506 of sedimentary units like the River and Term supersequences into normal faults oriented ENE-WSW
507 (Bradshaw et al., 2018;Gorton and Troup, 2018). Antiformal closures developed in the Punjaub Structure
508 and periclinal folds exposed just to its south at Mount Caroline and Ploughed Mountain share the same
509 ENE-WSW trend (Fig. 1b) and likely represent basin inversion structures formed during the same north-
510 south shortening event. However, as already pointed out, the Punjaub Structure is not a simple structure
511 and likely underwent limited folding before or subsequent to the start of deposition in the River and Term
512 supersequences (Gibson et al., 2020). Along with rocks of Calvert age in the core of the Punjaub Structure,
513 these two sequences were deformed during the 1650–1640 Ma Riversleigh Tectonic Event for which a NE-
514 SW shortening direction has been proposed (Gibson et al., 2020;Gibson et al., 2017). As such, shortening
515 during the earlier stages of basin inversion in the Punjaub Structure would have been approximately
516 orthogonal to strike in the Calvert Superbasin and its NW-SE basin-bounding normal faults. Seismic
517 sections oriented parallel to this shortening direction consistently show faults of Calvert age dipping
518 eastwards (e.g. Riversleigh Fault) and several have antiformal structures developed in their hangingwalls
519 (Figs. 8a & 8b) in accord with expectations that basin geometry prior to inversion was highly asymmetric
520 and had the form of a westward deepening half-graben. Westward deepening of Calvert-age extensional
521 basins on the Lawn Hill Platform is contrary to the results of earlier geophysical modelling (Betts et al.,
522 2004) indicating that half-graben of this age deepen southwards towards normal faults with NE orientations
523 essentially orthogonal to what is proposed here. However, while faults with this orientation have been
524 previously mapped (Hutton and Sweet, 1982) or have been known to exist in the subsurface for a long time
525 (Krassay et al., 2000a;Scott et al., 1998), it is debatable that they are of Calvert age or exercised any
526 significant control on depositional patterns during this phase of basin formation. They share the same NE
527 to ENE strike as normal faults in the Isa Superbasin and likely belong to the same generation of structures
528 that controlled deposition of the younger sedimentary basin. Importantly, faults of this age exhibit increased
529 amounts of throw southwards which would have been accompanied by commensurate amounts of
530 downward displacement in rocks of the underlying Calvert Superbasin, as captured in seismic images (Fig.
531 6a) along line 91Bn28–91Bn33 and the northern flank of the Punjaub Structure where the Loretta and Prize
532 supersequences, along with older elements of the Isa Superbasin, have been faulted downward by several
533 kilometres relative to their counterparts across the crest of the fold. This is the same stepped basin geometry
534 picked up in the results of geophysical modelling for the Lawn Hill Platform (Betts et al., 2004) and which,
535 during later crustal shortening, would have produced south-verging folds with the same NE axial direction
536 orientation as periclinal folds now observed at Mount Caroline and Ploughed Mountain (Fig. 1b). It further
537 follows that the NW-SE extensional direction previously proposed for the Calvert Superbasin more likely
538 relates to the younger Isa Superbasin and only came about because erosion across the Lawn Hill Platform
539 during or subsequent to the Isa Orogeny removed much of the younger basin infrastructure leaving behind
540 only the inverted and once more deeply buried rocks of the older basin.

541 West of the Lawn Hill Platform, crystalline basement lies at much shallower crustal depths and may even
542 have been exposed during deposition of the Georgina or South Nicholson basins, forming one or more
543 structural highs over the top of which there is a conspicuous thinning or draping of the younger cover rocks

(Fig. 9b). The older Paleoproterozoic–early Mesoproterozoic sequences are similarly notably thinner over basement in this region and the Calvert Superbasin may be entirely missing (Figs. 8b & 9b), either because it was never deposited or was removed by erosion during uplift accompanying the Riversleigh Tectonic Event. The River Supersequence consequently directly overlies a truncated and westward thinning older sequence taken here to be the Leichhardt Superbasin based on continuity with line 06GA–M2 (Fig. 8a) for which a stratigraphic interpretation has already been published. As with line 06GA–M2 (Fig. 8a), an angular unconformity separates the two sequences (see also Sweet, 1984), and the Leichhardt Superbasin had likely already been inverted before the River Supersequence was laid down. In keeping with this suggestion, the older sequence has locally been completely eroded away so that the River Supersequence rests directly on older crystalline basement (Fig. 8b). Moreover, even though a significant amount of this uplift and erosion may have been accommodated on reactivated older normal faults, the dominant structures in the seismic images are sub-vertical to steeply dipping and abruptly truncate stratigraphy not only in basement but thick basinal sequences developed in their footwalls. These footwall sequences encompass most if not all units of the Isa Superbasin (Figs. 8b & 9b), pointing to either a considerable amount of downward throw to the north on these structures or an equally significant amount of strike-slip displacement. The latter is thought more likely here consistent with the scale and abruptness of truncation and the observation that the faults overall have the character of flower-like structures (Fig. 9b). Such uncertainties aside, it seems reasonable to conclude that basement uplift on these subvertical faults occurred late as these structures displace all units in the Isa Superbasin and cut up-section all the way to the base of the Cambrian. Faults with similarly steep attitudes and character are also evident in north-south oriented seismic sections (Fig. 6) for the northern Lawn Hill Platform (e.g. 91Bn28–91Bn33) and likely belong to the same generation of strike-slip faults. Significantly, they share the same NE to ENE strike and were possibly initiated on older structures dating back to formation of the Isa Superbasin into which they root downward (Fig. 6a). Late NE-trending strike-slip faulting has recently been attributed to the onset of extensional collapse and orogen-parallel extrusion of thermally weakened crust following arc-continent or continent-continent collision between Australia and Laurentia (Gibson et al., 2020).

4.2 Basin inversion and implications for Pb–Zn mineralisation

As revealed in seismic sections oriented orthogonal to one another, basin inversion in the north Australian Paleoproterozoic–Mesoproterozoic sequences occurred on more than one occasion and gave rise to a structural architecture not unlike that recorded in basins of much younger age such as the Irish and North seas and North Atlantic petroleum province more generally. No less important in this context are the results of past and recent drilling confirming that northern Australia is prospective for oil and gas (Gorton and Troup, 2018; Jackson et al., 1986; McConachie et al., 1993), not all of which has its source in the South Nicholson or younger sedimentary basins (Glikson et al., 2006; Golding et al., 2006). Some is known to be considerably older (Jackson et al., 1986) or at least date back to the time of Pb–Zn mineralisation in the 1575 Ma Century deposit (Broadbent et al., 1998). Bituminous residues occur widely throughout this deposit (Broadbent et al., 1998) and more recent studies have shown that carbonaceous shales and dolomitic siltstones hosting the ore body (Wide Supersequence) contain exceptionally high levels of total organic carbon, along with other parts of the Isa Superbasin (Glikson et al., 2006; Gorton and Troup, 2018; Jarrett et al., 2018). However, this need not imply that the mineralising fluids were emplaced into an existing oil or gas reservoir as required by the Broadbent et al. (1998) model for ore formation. An alternative possibility is that the organic matter was already present in the host rocks from the time they were deposited and got transformed into oil and/or gas during ingress of the mineralising fluid itself (Glikson et al., 2006; Golding et al., 2006). Either way, it is difficult to avoid the conclusion that a petroleum system was in operation during or immediately prior to mineralisation. Moreover, if fluid:rock ratios were high at the time of mineralisation, much of the organic carbon would have been removed from the deposit site, leaving behind

590 bituminous residues but more importantly leading to transient increases in pore space that was subsequently
591 filled by sulphides (Glikson et al., 2006). Stable isotope studies combined with analyses of illite crystallinity
592 and organic reflectance would further indicate that this processes occurred under a normal thermal gradient
593 (ca. $24^{\circ}\text{Ckm}^{-1}$) and temperatures below 200°C (Glikson et al., 2006;Golding et al., 2006) and thus without
594 the need for additional magmatic or metamorphic heating. Bimodal magmatism ceased some 60–70 Myr
595 earlier at ca. 1655 Ma and so any related thermal anomaly would have long since decayed and been
596 unavailable to drive either fluid flow or the mineralisation process. Instead, any extraneous heat added to
597 the system may have come from the hydrothermal fluids themselves whose expulsion from deeper levels
598 of the basin was more likely driven by a build-up of fluid overpressures as the twin processes of crustal
599 shortening and basin inversion took effect.

600 Significantly, a near-identical scenario have been proposed for some carbonate-hosted Pb–Zn deposits of
601 Mississippi Valley-type (Leach et al., 2001;Leach et al., 2010) which nearly always contain some amount
602 of pyrobitumen or organic carbon and may similarly have formed through mixing of hydrocarbons with a
603 hydrothermal metal-bearing fluid (Anderson, 2008;Kesler et al., 1994). Such similarities with Century and
604 the clastic-dominated Pb–Zn deposits of northern Australia have been noted before (Huston et al., 2006)
605 but are usually tempered by perceived differences in tectonic setting or the timing of mineralisation relative
606 to orogenesis. A compressional foreland setting is usually advanced for the former (Leach et al., 2001)
607 whereas the Pb–Zn deposits of northern Australia are thought to be largely syn-extensional in origin and
608 form prior to the onset of orogenesis (Huston et al., 2006;Large et al., 2005). In the interpretation presented
609 here, there is no discernible difference in tectonic setting between the two different deposit styles, and late
610 Paleoproterozoic-early Mesoproterozoic Pb–Zn mineralisation at Century and elsewhere across the region
611 was driven by basin inversion linked to orogenesis and crustal shortening (Gibson et al., 2020;Gibson et
612 al., 2017) as originally envisaged by Broadbent et al. (1998).

613 Moreover, in view of seismic evidence for basin inversion towards the end of Calvert time (e.g. Fig. 6a),
614 there is no reason why the Walford Creek Pb–Zn deposit (Rohrlach et al., 1998) located just to the north of
615 Century (Fig. 1a) could not have formed under similar circumstances. Although older, and hosted by
616 carbonate rocks of the Loretta Supersequence (Walford Dolomite), its host rocks were similarly laid down
617 during a period of increasing tectonic instability (Riversleigh Tectonic Event). The deposit itself has also
618 been described as being of Mississippi Valley-type (Rohrlach et al., 1998). No less importantly, fluid
619 inclusions from this ore body are known to contain light oil (Rohrlach et al., 1998), most likely sourced and
620 introduced ahead of mineralisation from shales rich in organic carbon (Mount Les Siltstone) in the overlying
621 River Supersequence (Glikson et al., 2006). Thus, not only were hydrocarbons leaking from one
622 stratigraphic unit into another in this region but there is a strong possibility that a petroleum system was
623 present up to and possibly including the time of mineralisation. Accordingly, as at Century, the mineralising
624 fluid may have interacted or mixed with organic carbon, making for a highly reducing environment into
625 which more oxidised metal-bearing fluids were introduced, and doubly so if the hydrocarbon fluid was
626 contaminated by sour gas and contained appreciable amounts of hydrogen sulphide as is often the case with
627 Mississippi Valley-type Pb–Zn deposits (Anderson, 2008;Huston et al., 2006). On encountering this
628 reducing environment, a number of catalysed redox reactions ensued during the course of which existing
629 carbonate minerals were dissolved and metal sulphides precipitated in their place. Metal precipitation in
630 other Pb–Zn deposits across the region, including Mount Isa, was likely driven by similar replacement
631 reactions following upward transport of metalliferous fluids sourced from deeper levels of the basin. Fluids
632 may initially have travelled up reactivated faults but on arrival at the ore formation site became trapped and
633 migrated into their hangingwalls or footwall shortcut thrusts where they brought about dissolution of the
634 host rock and its replacement by sulphides. This compares with current ore formation models where the
635 mineralising fluid was introduced along basin-bounding structures active at the time of basin formation

(Huston et al., 2006; Large et al., 2005; McGoldrick et al., 2010; Southgate et al., 2000b) or along normal faults reactivated in the opposite sense during periods of transient crustal shortening in an overall extensional or sag setting (Betts et al., 2003; Kunzmann et al., 2019). Mineral exploration has accordingly often been directed towards the identification of structures and sedimentary sequences formed during the course of basin formation as opposed to those that may have formed during later basin inversion.

However, as is now evident from recent seismic interpretations of line 06GA-M2 (Gibson et al., 2017; Gibson et al., 2016), the carbonaceous rocks hosting Century belong to the syn-inversion fraction of basin fill and were deposited at a time of crustal shortening accompanying the Isan Orogeny. There is no evidence that this shortening was accompanied by reactivation of the basin-bounding structure. Instead, as with many normal faults, the Riversleigh Fault dipped too steeply to be easily reactivated and strain was taken up on a footwall shortcut thrust; it rather than the Riversleigh Fault would have served as the better fluid conduit. Interestingly, the Termite Range Fault has some of the same attributes as a footwall shortcut thrust and is widely believed (Broadbent et al., 1998; Yang and Radulescu, 2006) to have been the main fluid conduit for the Century deposit which lies either above or in a minor offshoot immediately adjacent to the master structure. No less importantly, mineralisation is transgressive with respect to stratigraphy and occurred through replacement processes (Broadbent et al., 1998), consistent with the 1575 Ma age reported for this deposit (Carr et al., 2004). This is long after the start of crustal shortening and probable concomitant expulsion of hydrocarbons to higher stratigraphic levels where they would have pooled or been trapped in structures formed during inversion. It seems further likely, if the analogy with the petroleum system has any validity, that a significant amount of this metal-bearing fluid found its way into the same type of hangingwall structures that are so prospective of oil and gas in the younger inverted basins of the North Atlantic petroleum province. If this is indeed the case, then a change in exploration strategies for sediment-hosted Pb-Zn mineralisation may be warranted where there is less focus on the identification of normal faults active at the time of basin formation towards increased targeting of potential structural traps located in either the footwalls or less proximal parts of their inverted hangingwall structures.

Importantly, owing to asymmetries inherited from the original basin architecture, the default position for the latter will be the same regions where basin fill attained maximum thickness and source rocks were sufficiently deeply buried to generate the requisite volumes of metalliferous fluids during basin inversion. Potential source rocks for Pb and Zn metal include the syn-rift component of basin fill which, in these regions, might be expected to include thick sequences of altered volcanic and immature sedimentary rocks as was reportedly the case for mineral deposits in the McArthur Basin and Leichhardt River Fault Trough (Cooke et al., 1998; Heinrich et al., 1995; Huston et al., 2016; Huston et al., 2006; Polito et al., 2006; Southgate et al., 2006). However, as revealed by the seismic data, substantial amounts of the Calvert and Leichhardt superbasins were removed through erosion during inversion so that neither the full complement of syn-rift rocks nor any vestige of a basin seal need be preserved in one or both basins (e.g. 17GA-SN1 and SN2). Basin seals and barriers to upward fluid flow are more likely to be found among the finer-grained carbonaceous shales and dolomitic siltstones making up the post-rift fraction of basin fill but this is the very component most susceptible to uplift and erosion during the initial stages of basin inversion. Accordingly, the optimal site for the formation and preservation of Pb-Zn mineralisation may be in basins whose inverted hangingwalls and related structures never lost all of their post-rift capping rocks and continued to evolve beneath succeeding layers of tectonically-driven sedimentation. In either event, it is difficult to avoid the conclusion that basin inversion played an important, if not critical, role in the formation of a world-class Pb-Zn mineral province in northern Australia.

5 Acknowledgements

680 For the invitation and opportunity to contribute to the special anniversary volume on basin inversion we
681 thank editors, professors Jonas Kley and Piotr Krzywiec. For detailed and comprehensive reviews that
682 greatly improved the text we are indebted to Professor Alan Collins and Dr Karen Connors. Thanks also
683 to Teck Resources Australia and Pursuit Minerals for permission to publish our interpretation of the
684 Punjab Structure. Figure 2 was produced on our behalf by Dr Ian Withnall, Geological Survey of
685 Queensland. Seismic reflection data on which this paper depends are available online from their
686 respective data repositories: (Geoscience Australia eCat: <http://pid.geoscience.gov.au/dataset/ga/69674>)
687 and Queensland Geological Survey:
688 <https://qdexdata.dnrme.qld.gov.au/QDEXDataDownloadManager/Results?type=Seismic&id=95456,95541,91004>.
689

690 **6 References**

- 691 Ahmad, M., and Munson, T. J.: Chapter 18: Lawn hill platform, in: *Geology and mineral resources of the Northern*
692 *Territory, Special Publication 5*, edited by: Ahmad, M., and Munson, T. J., Northern Territory Geological Survey,
693 Darwin, 2013.
- 694 Anderson, G. M.: The mixing hypothesis and the origin of Mississippi Valley-type deposits, *Economic Geology*, 103,
695 1683-1690, 2008.
- 696 Andrews, S. J.: Stratigraphy and depositional setting of the upper McNamara group, Lawn Hill region, northwest
697 Queensland, *Economic Geology*, 93, 1132-1152, [10.2113/gsecongeo.93.8.1132](https://doi.org/10.2113/gsecongeo.93.8.1132), 1998.
- 698 Baker, M. J., Crawford, A. J., and Withnall, I. W.: Geochemical, Sm-Nd isotopic characteristics and petrogenesis of
699 Paleoproterozoic mafic rocks from the Georgetown Inlier, north Queensland: Implications for relationship with
700 the Broken Hill and Mount Isa eastern succession, *Precambrian Research*, 177, 39-54, 2010.
- 701 Betts, P. G., and Lister, G. S.: Comparison of the 'strike-slip' versus the 'episodic rift-sag' models for the origin of
702 the Isa Superbasin, *Australian Journal of Earth Sciences*, 48, 265 - 280, 2001.
- 703 Betts, P. G., Giles, D., and Lister, G. S.: Tectonic environment of shale-hosted massive sulphide Pb-Zn-Ag deposits
704 of Proterozoic northeastern Australia, *Economic Geology*, 98, 557-576, 2003.
- 705 Betts, P. G., Giles, D., and Lister, G. S.: Aeromagnetic patterns of half-graben and basin inversion: Implications for
706 sediment-hosted massive sulfide Pb-Zn-Ag exploration, *Journal of Structural Geology*, 26, 1137-1156,
707 <http://dx.doi.org/10.1016/j.jsg.2003.11.020>, 2004.
- 708 Betts, P. G., and Giles, D.: The 1800-1100 Ma tectonic evolution of Australia, *Precambrian Research*, 144, 92-125,
709 2006.
- 710 Betts, P. G., Giles, D., Mark, G., Lister, G. S., Goleby, B. R., and Ailleres, L.: Synthesis of the Proterozoic evolution of
711 the Mount Isa inlier, *Australian Journal of Earth Sciences*, 53, 187-211, 2006.
- 712 Betts, P. G., Armit, R. J., Stewart, J., Aitken, A. R. A., Ailleres, L., Donchak, P., Hutton, L., Withnall, I., and Giles, D.:
713 *Australia and Nuna*, Geological Society, London, Special Publications, 424, 47-81, [10.1144/sp424.2](https://doi.org/10.1144/sp424.2), 2016.
- 714 Bierlein, F. P., Black, L. P., Hergt, J., and Mark, G.: Evolution of pre-1.8 Ga basement rocks in the western Mt Isa
715 inlier, northeastern Australia--insights from shrimp U-Pb dating and in-situ Lu-Hf analysis of zircons, *Precambrian*
716 *Research*, 163, 159-173, 2008.
- 717 Bierlein, F. P., Maas, R., and Woodhead, J.: Pre-1.8 Ga tectono-magmatic evolution of the Kalkadoon-Leichhardt
718 belt: Implications for the crustal architecture and metallogeny of the Mount Isa inlier, northwest Queensland,
719 Australia, *Australian Journal of Earth Sciences*, 58, 887-915, [10.1080/08120099.2011.571286](https://doi.org/10.1080/08120099.2011.571286), 2011.
- 720 Black, L. P., and McCulloch, M. T.: Isotopic evidence for the dependence of recurrent felsic magmatism on new
721 crust formation: An example from the Georgetown region of northeastern Australia, *Geochimica et Cosmochimica*
722 *Acta*, 54, 183-196, 1990.
- 723 Black, L. P., Gregory, P., Withnall, I. W., and Bain, J. H. C.: U-Pb zircon age for the Etheridge Group, Georgetown
724 region, north Queensland: Implications for relationship with the Broken Hill and Mt Isa sequences, *Australian*
725 *Journal of Earth Sciences*, 45, 925 - 935, 1998.
- 726 Blaikie, T. N., Betts, P. G., Armit, R. J., and Ailleres, L.: The ca. 1740–1710 Ma Leichhardt Event: Inversion of a
727 continental rift and revision of the tectonic evolution of the north Australian craton, *Precambrian Research*, 292,
728 75-92, <http://dx.doi.org/10.1016/j.precamres.2017.02.003>, 2017.
- 729 Blake, D. H.: *Geology of the Mount Isa inlier and environs, Queensland and Northern Territory*, BMR Bulletin, 225,
730 83, 1987.

731 Bradshaw, B. E., and Scott, D. J.: Integrated basin analysis of the Isa Superbasin using seismic, well-log and
732 geopotential data: An evaluation of the economic potential of the northern Lawn Hill Platform, Australian
733 Geological Survey Organisation (now Geoscience Australia) AGSO Record 199/19 (Digital Version), Canberra,
734 1999.

735 Bradshaw, B. E., Lindsay, J. F., Krassay, A. A., and Wells, A. T.: Attenuated basin-margin sequence stratigraphy of
736 the Palaeoproterozoic Calvert and Isa superbasins: The Fickling Group, southern Murphy Inlier, Queensland,
737 Australian Journal of Earth Sciences, 47, 599 - 623, 2000.

738 Bradshaw, B. E., Orr, M. L., Bailey, A. H. E., Palu, T. J., and Hall, L. S.: Northern Lawn Hill Platform: Depth, structure
739 and isochore mapping update, Geoscience Australia Record 2018/47, 75pp, Geoscience Australia, Canberra, 2018.

740 Broadbent, G. C., Myers, R. E., and Wright, J. V.: Geology and origin of shale-hosted Zn-Pb-Ag mineralization at the
741 Century deposit, northwest Queensland, Australia, Economic Geology, 93, 1264-1294,
742 10.2113/gsecongeo.93.8.1264, 1998.

743 Carr, G. R., Denton, G. J., Parr, J., Sun, S.-S., Korsch, R. J., and Boden, S. B.: Lightning does strike twice; multiple ore
744 events in major mineralised systems in northern Australia, in: Predictive mineral discovery under cover, extended
745 abstracts, edited by: Muhling, J., Goldfarb, R., Vielreicher, N., Bierlein, F., Stumpfl, E., Groves, D. I., and
746 Kenworthy, S., Centre for Global Metallogeny, The University of Western Australia, Perth, 2004.

747 Carr, L. K., Southby, C., Henson, P., Costelloe, R., Anderson, J. R., Jarrett, A. J. M., Carson, C. J., MacFarlane, S. K.,
748 Gorton, J., Hutton, L. J., Troup, A., Williams, B., Khider, K., Bailey, A. H. E., and Fomin, T.: Exploring for the future:
749 South Nicholson Basin geological summary and seismic data interpretation. Record 2019/21., Geoscience
750 Australia, Canberra, 2019.

751 Cooke, D. R., Bull, S. W., Donovan, S., and Rogers, J. R.: K-metasomatism and base metal depletion in volcanic
752 rocks from the McArthur basin, Northern Territory—implications for base metal mineralization, Economic Geology,
753 93, 1237–1263, 1998.

754 Cooper, M. A., Collins, D., Ford, M., Murphy, F. X., and Trayner, P. M.: Structural style, shortening estimates and
755 the thrust front of the Irish Variscides, Geological Society, London, Special Publications, 14, 167-175,
756 10.1144/gsl.sp.1984.014.01.16, 1984.

757 Cooper, M. A., Williams, G. D., de Graciansky, P. C., Murphy, R. W., Needham, T., de Paor, D., Stoneley, R., Todd, S.
758 P., Turner, J. P., and Ziegler, P. A.: Inversion tectonics — a discussion, Geological Society, London, Special
759 Publications, 44, 335-347, 10.1144/gsl.sp.1989.044.01.18, 1989.

760 Domagala, J., Southgate, P. N., McConachie, B. A., and Pidgeon, B. A.: Evolution of the Palaeoproterozoic Prize,
761 Gun and lower Loretta supersequences of the Surprise Creek Formation and Mt Isa group, Australian Journal of
762 Earth Sciences, 47, 485 - 507, 2000.

763 Dooley, T., and McClay, K. R.: Analog modeling of pull-apart basins, AAPG Bulletin, 81, 1804-1826, 1997.

764 Duncan, R. J., Stein, H. J., Evans, K. A., Hitzman, M. W., Nelson, E. P., and Kirwin, D. J.: A new geochronological
765 framework for mineralization and alteration in the Selwyn-Mount Dore corridor, eastern fold belt, Mount Isa
766 inlier, Australia: Genetic implications for iron oxide copper-gold deposits, Economic Geology, 106, 169-192,
767 10.2113/econgeo.106.2.169, 2011.

768 Foster, D. R. W., and Rubenach, M.: Isograd patterns and regional low-pressure- high-temperature metamorphism
769 of pelitic, mafic and calc-silicate rocks along an east-west section through the Mount Isa inlier, Australian Journal
770 of Earth Sciences, 53, 167-186, 2006.

771 Foster, D. R. W., and Austin, J. R.: The 1800–1610 Ma stratigraphic and magmatic history of the eastern
772 succession, Mount Isa inlier, and correlations with adjacent Paleoproterozoic terranes, Precambrian Research,
773 163, 7-30, <http://dx.doi.org/10.1016/j.precamres.2007.08.010>, 2008.

774 Frogtech Geoscience: North West Queensland SEEBASE® Study and GIS. Queensland Geological Record 2018/03,
775 2018.

776 Gibson, G. M., Rubenach, M. J., Neumann, N. L., Southgate, P. N., and Hutton, L. J.: Syn- and post-extensional
777 tectonic activity in the Palaeoproterozoic sequences of Broken Hill and Mount Isa and its bearing on
778 reconstructions of Rodinia, Precambrian Research, 166, 350-369,
779 <http://dx.doi.org/10.1016/j.precamres.2007.05.005>, 2008.

780 Gibson, G. M., Henson, P. A., Neumann, N. L., Southgate, P. N., and Hutton, L. J.: Paleoproterozoic-earliest
781 Mesoproterozoic basin evolution in the Mount Isa region, northern Australia and implications for reconstructions
782 of the Nuna and Rodinia supercontinents, Episodes, 35, 131-141, 2012.

783 Gibson, G. M., Meixner, A. J., Withnall, I. W., Korsch, R. J., Hutton, L. J., Jones, L. E. A., Holzschuh, J., Costelloe, R.
784 D., Henson, P. A., and Saygin, E.: Basin architecture and evolution in the Mount Isa mineral province, northern
785 Australia: Constraints from deep seismic reflection profiling and implications for ore genesis, *Ore Geology*
786 *Reviews*, 76, 414-441, <http://dx.doi.org/10.1016/j.oregeorev.2015.07.013>, 2016.

787 Gibson, G. M., Hutton, L. J., and Holzschuh, J.: Basin inversion and supercontinent assembly as drivers of
788 sediment-hosted Pb–Zn mineralization in the Mount Isa region, northern Australia, *Journal of the Geological*
789 *Society*, 174, 773-786, 10.1144/jgs2016-105, 2017.

790 Gibson, G. M., Champion, D. C., Withnall, I. W., Neumann, N. L., and Hutton, L. J.: Assembly and breakup of the
791 Nuna supercontinent: Geodynamic constraints from 1800 to 1600 Ma sedimentary basins and basaltic
792 magmatism in northern Australia, *Precambrian Research*, 313, 148-169,
793 <https://doi.org/10.1016/j.precamres.2018.05.013>, 2018.

794 Gibson, G. M., Champion, D. C., Huston, D. L., and Withnall, I. W.: Orogenesis in Paleo-Mesoproterozoic eastern
795 Australia: A response to arc-continent and continent-continent collision during assembly of the Nuna
796 supercontinent, *Tectonics*, 39, e2019TC005717, 10.1029/2019tc005717, 2020.

797 Giles, D., Betts, P. G., and Lister, G. S.: Far-field continental back-arc setting for the 1.8-1.67 Ma basins of north-
798 east Australia, *Geology*, 30, 823-826, 2002.

799 Giles, D., Betts, P. G., and Lister, G. S.: 1.8–1.5-ga links between the North and South Australian cratons and the
800 early–middle Proterozoic configuration of Australia, *Tectonophysics*, 380, 27-41,
801 <http://dx.doi.org/10.1016/j.tecto.2003.11.010>, 2004.

802 Giles, D., Betts, P. G., Ailleres, L., Hulscher, B., Hough, M., and Lister, G. S.: Evolution of the Isan Orogeny at the
803 southeastern margin of the Mt Isa inlier, *Australian Journal of Earth Sciences*, 53, 91-108, 2006.

804 Glikson, A. Y., Derrick, G. M., Wilson, I. H., and Hill, R. M.: Tectonic evolution and crustal setting of the middle
805 Proterozoic Leichhardt River Fault Trough, Mount Isa region, northwest Queensland, *BMR Journal of Australian*
806 *Geology and Geophysics*, 1, 115-129, 1976.

807 Glikson, M., Golding, S. D., and Southgate, P. N.: Thermal evolution of the ore-hosting Isa Superbasin: Central and
808 northern Lawn Hill Platform, *Economic Geology*, 101, 1211-1229, 10.2113/gsecongeo.101.6.1211, 2006.

809 Golding, S. D., Uysal, I. T., Glikson, M., Baublys, K. A., and Southgate, P. N.: Timing and chemistry of fluid-flow
810 events in the Lawn Hill Platform, northern Australia, *Economic Geology*, 101, 1231-1250,
811 10.2113/gsecongeo.101.6.1231, 2006.

812 Gorton, J., and Troup, A.: Petroleum systems of the Proterozoic in northwest Queensland and a description of
813 various play types, *The APPEA Journal*, 58, 311-320, <https://doi.org/10.1071/AJ17115>, 2018.

814 Hayward, A. B., and Graham, R. H.: Some geometrical characteristics of inversion, Geological Society, London,
815 *Special Publications*, 44, 17-39, 10.1144/gsl.sp.1989.044.01.03, 1989.

816 Heinrich, C. A., Bain, J. H. C., Mernagh, T. P., Wyborn, L. A. I., Andrew, A. S., and Waring, C. L.: Fluid and mass
817 transfer during metabasalt alteration and copper mineralisation at Mount Isa, Australia, *Economic Geology*, 90,
818 705-730, 1995.

819 Hinman, M.: Base metal mineralisation at McArthur River: Structure and kinematics of the HYC-Cooley Zone,
820 *Australian Geological Survey Organisation Record* 1995/5, 41pp, 1995.

821 Holcombe, R. J., Pearson, P. J., and Oliver, N. H. S.: Geometry of a middle Proterozoic extensional decollement in
822 north-eastern Australia, *Tectonophysics*, 191, 255-274, 1991.

823 Huston, D. L., Stevens, B., Southgate, P. N., Muhling, P., and Wyborn, L.: Australian Zn-Pb-Ag ore-forming systems:
824 A review and analysis, *Economic Geology*, 101, 1117-1157, 10.2113/gsecongeo.101.6.1117, 2006.

825 Huston, D. L., Mernagh, T. P., Hagemann, S. G., Doublier, M. P., Fiorentini, M., Champion, D. C., Lynton Jaques, A.,
826 Czarnota, K., Cayley, R., Skirrow, R., and Bastrakov, E.: Tectono-metallogenic systems — the place of mineral
827 systems within tectonic evolution, with an emphasis on Australian examples, *Ore Geology Reviews*, 76, 168-210,
828 <http://dx.doi.org/10.1016/j.oregeorev.2015.09.005>, 2016.

829 Hutton, L. J., and Sweet, I. P.: Geological evolution, tectonic style and economic potential of the Lawn Hill Platform
830 cover, northwest Queensland, *BMR Journal of Australian Geology and Geophysics*, 7, 125-134, 1982.

831 Jackson, M. J., Powell, T. G., Summons, R. E., and Sweet, I. P.: Hydrocarbon shows and petroleum source rocks in
832 sediments as old as 1.7×10^9 years, *Nature*, 322, 727-729, 10.1038/322727a0, 1986.

833 Jackson, M. J., Scott, D. L., and Rawlings, D. J.: Stratigraphic framework for the Leichhardt and Calvert superbasins:
834 Review and correlations of the pre- 1700 Ma successions between Mt Isa and McArthur River, Australian Journal
835 of Earth Sciences, 47, 381-403, 10.1046/j.1440-0952.2000.00789.x, 2000.

836 Jarrett, A. J. M., Cox, G. M., Southby, C., Hong, Z., Palatty, P., Carr, L., and Henson, P.: Source rock geochemistry of
837 the McArthur basin, northern Australia: Rock-eval pyrolysis data release. Record 2018/24. Geoscience Australia,
838 Canberra, <http://dx.doi.org/10.11636/Record.2018.024>, 2018.

839 Kesler, S. E., Jones, H. D., Furman, F. C., Sassen, R., Anderson, W. H., and Kyle, J. R.: Role of crude oil in the genesis
840 of Mississippi Valley-type deposits: Evidence from the Cincinnati Arch, *Geology*, 22, 609-612, 10.1130/0091-
841 7613(1994)022<0609:rocoit>2.3.co;2, 1994.

842 Korsch, R. J., Huston, D. L., Henderson, R. A., Blewett, R. S., Withnall, I. W., Fergusson, C. L., Collins, W. J., Saygin,
843 E., Kositcin, N., Meixner, A. J., Chopping, R., Henson, P. A., Champion, D. C., Hutton, L. J., Wormald, R., Holzschuh,
844 J., and Costelloe, R. D.: Crustal architecture and geodynamics of north Queensland, Australia: Insights from deep
845 seismic reflection profiling, *Tectonophysics*, 572–573, 76-99, <http://dx.doi.org/10.1016/j.tecto.2012.02.022>, 2012.

846 Kositcin, N., and Carson, C. J.: New shrimp U–Pb zircon ages from the South Nicholson and Carrara Range region,
847 Northern Territory. Record 2019/09. Geoscience Australia, Canberra., 2019.

848 Krassay, A. A., Bradshaw, B. E., Domagala, J., and Jackson, M. J.: Siliciclastic shoreline to growth-faulted, turbiditic
849 sub-basins: The Proterozoic River Supersequence of the upper McNamara Group on the Lawn Hill Platform,
850 northern Australia, *Australian Journal of Earth Sciences*, 47, 533 - 562, 2000a.

851 Krassay, A. A., Domagala, J., Bradshaw, B. E., and Southgate, P. N.: Lowstand ramps, fans and deep-water
852 Palaeoproterozoic and Mesoproterozoic facies of the Lawn Hill Platform: The Term, Lawn, Wide and Doom
853 supersequences of the Isa Superbasin, northern Australia, *Australian Journal of Earth Sciences*, 47, 563 - 597,
854 2000b.

855 Kunzmann, M., Schmid, S., Blaikie, T. N., and Halverson, G. P.: Facies analysis, sequence stratigraphy, and carbon
856 isotope chemostratigraphy of a classic Zn-Pb host succession: The Proterozoic middle McArthur Group, McArthur
857 Basin, Australia, *Ore Geology Reviews*, 106, 150-175, <https://doi.org/10.1016/j.oregeorev.2019.01.011>, 2019.

858 Large, R. R., Bull, S. W., McGoldrick, P. J., Walters, S., Derrick, G. M., and Carr, G. R.: Stratiform and strata-bound
859 Zn-Pb-Ag deposits in Proterozoic sedimentary basins, northern Australia, *Economic Geology 100th Anniversary*
860 *Volume*, 931-963, 2005.

861 Leach, D. L., Bradley, D., Lewchuk, M. T., Symons, D. T., de Marsily, G., and Brannon, J.: Mississippi Valley-type
862 lead–zinc deposits through geological time: Implications from recent age-dating research, *Miner Deposita*, 36,
863 711-740, 10.1007/s001260100208, 2001.

864 Leach, D. L., Bradley, D. C., Huston, D., Pisarevsky, S. A., Taylor, R. D., and Gardoll, S. J.: Sediment-hosted lead-zinc
865 deposits in earth history, *Economic Geology*, 105, 593-625, 10.2113/gsecongeo.105.3.593, 2010.

866 Lowell, J. D.: Mechanics of basin inversion from worldwide examples, Geological Society, London, Special
867 Publications, 88, 39-57, 10.1144/gsl.sp.1995.088.01.04, 1995.

868 Martínez, F., Arriagada, C., Mpodozis, C., and Peña1, M.: The Lautaro Basin: A record of inversion tectonics in
869 northern Chile, *Andean Geology*, 39, 258-278, 2012.

870 McClay, K. R.: The geometries and kinematics of inverted fault systems: A review of analogue model studies,
871 Geological Society, London, Special Publications, 88, 97-118, 10.1144/gsl.sp.1995.088.01.07, 1995.

872 McClay, K. R., and White, M. J.: Analogue modelling of orthogonal and oblique rifting, *Marine and Petroleum*
873 *Geology*, 12, 137-151, 1995.

874 McClay, K. R., Dooley, T., Whitehouse, P., and Mills, M.: 4-D evolution of rift systems: Insights from scaled physical
875 models, *AAPG Bulletin*, 86, 935-959, 10.1306/61eedbf2-173e-11d7-8645000102c1865d, 2002.

876 McConachie, B. A., Barlow, M. G., Dunster, J. N., Meaney, R. A., and Schaap, A. D.: The Mount Isa basin-definition,
877 structure and petroleum geology, *APEA Journal*, 33, 237-257, 1993.

878 McConachie, B. A., and Dunster, J. N.: Sequence stratigraphy of the Bowthorn block in the northern Mount Isa
879 basin, Australia: Implications for the base-metal mineralization process, *Geology*, 24, 155-158, 10.1130/0091-
880 7613(1996)024<0155:ssotbb>2.3.co;2, 1996.

881 McGoldrick, P., Winefield, P., Bull, S., Selley, D., and Scott, R. J.: Sequences, synsedimentary structures, and sub-
882 basins: The where and when of sedex zinc systems in the southern McArthur Basin, Australia, *Society of Economic*
883 *Geologists, Special Publication 15*, 367–389, 2010.

884 Neumann, N. L., Southgate, P. N., Gibson, G. M., and McIntyre, A.: New shrimp geochronology for the western
885 fold belt of the Mount Isa inlier: Developing a 1800–1650 Ma event framework, *Australian Journal of Earth
886 Sciences*, 53, 1023-1039, 2006.

887 Neumann, N. L., Gibson, G. M., and Southgate, P. N.: New shrimp age constraints on the timing and duration of
888 magmatism and sedimentation in the Mary Kathleen Fold Belt, Mt Isa inlier, *Australian Journal of Earth Sciences*,
889 56, 965-983, 2009.

890 O'Dea, M. G., Lister, G. S., Betts, P. G., and Pound, K. S.: A shortened intraplate rift system in the Proterozoic
891 Mount Isa terrane, N. W. Queensland, Australia, *Tectonics*, 16, 425-441, 1997a.

892 O'Dea, M. G., Lister, G. S., MacCready, T., Betts, P. G., Oliver, N. H. S., Pound, K. S., Huang, W., Valenta, R. K.,
893 Oliver, N. H. S., and Valenta, R. K.: Geodynamic evolution of the Proterozoic Mount Isa terrain, *Geological Society,
894 London, Special Publications*, 121, 99-122, 10.1144/gsl.sp.1997.121.01.05, 1997b.

895 Page, R. W., and Sun, S. S.: Aspects of geochronology and crustal evolution in the eastern fold belt, Mt Isa inlier,
896 *Australian Journal of Earth Sciences*, 45, 343-361, 10.1080/08120099808728396, 1998.

897 Page, R. W., Jackson, M. J., and Krassay, A. A.: Constraining sequence stratigraphy in north Australian basins:
898 Shrimp U-Pb zircon geochronology between Mt Isa and McArthur River, *Australian Journal of Earth Sciences*, 47,
899 431 - 459, 2000.

900 Pearson, P. J., Holcombe, R. J., and Page, R. W.: Synkinematic emplacement of the middle Proterozoic Wonga
901 Batholith into a midcrustal shear zone, Mount Isa inlier, Queensland, Australia, in: *Detailed studies of the Mount
902 Isa inlier: Australian geological survey organisation bulletin 243*, edited by: Stewart, A. J., and Blake, D. H.,
903 Canberra, 289-328, 1991.

904 Polito, P. A., Kyser, T. K., Golding, S., D., and Southgate, P. N.: Zinc deposits and related mineralization of the
905 Burketown mineral field, including the world-class Century deposit, northern Australia: Fluid inclusion and stable
906 isotope evidence for basin fluid sources, *Economic Geology*, 101, 1251-1273, 10.2113/gsecongeo.101.6.1251,
907 2006.

908 Pollard, P., and McNaughton, N. J.: U/Pb geochronology and Sm/Nd isotope characterization of Proterozoic
909 intrusive rocks in the Cloncurry district, Mount Isa inlier, Australia. *Amira P438 Cloncurry base metals and gold
910 final report: Section 4*, 19pp., 1997.

911 Pollard, P. J., Mark, G., and Mitchell, L. C.: Geochemistry of post-1540 Ma granites spatially associated with
912 regional sodic-calcic alteration and Cu-Au-Co mineralisation, Cloncurry district, northwest Queensland *Economic
913 Geology*, 93, 1330-1344, 1998.

914 Pourteau, A., Smit, M. A., Li, Z.-X., Collins, W. J., Nordvan, A. R., Volante, S., and Li, J.: 1.6 Ga crustal thickening
915 along the final Nuna suture, *Geology*, 46, 959-962, 10.1130/G45198.1, 2018.

916 Pursuit Minerals: Pursuit minerals limited lists on ASX and immediately commences Bluebush drilling program.
917 [Http://pursuitminerals.Com.Au/wp-content/uploads/2017/09/pur-lists-on-ASX-and-commences-bluebush-
918 drilling-program.Pdf](http://pursuitminerals.com.au/wp-content/uploads/2017/09/pur-lists-on-ASX-and-commences-bluebush-drilling-program.pdf), 2017.

919 Rawlings, D. J., Sweet, I. P., and Kruse, P. D.: Mount Drummond, Northern Territory. 1:250 000 geological map
920 series explanatory notes, Se 53-12. Northern Territory Geological Survey, Darwin, 2008.

921 Rohrlach, B. D., Fu, M., and Clarke, J. D. A.: Geological setting, paragenesis and fluid history of the Walford Creek
922 Zn-Pb-Cu-Ag prospect, Mt Isa basin, Australia, *Australian Journal of Earth Sciences*, 45, 63-81,
923 10.1080/08120099808728367, 1998.

924 Rubenach, M. J., Foster, D. R. W., Evins, P. M., Blake, K. L., and Fanning, C. M.: Age constraints on the
925 tectonothermal evolution of the Selwyn zone, eastern fold belt, Mount Isa inlier, *Precambrian Research*, 163, 81-
926 107, 2008.

927 Scott, D. L., Bradshaw, B. E., and Tarlowski, C. Z.: The tectonostratigraphic history of the Proterozoic northern
928 Lawn Hill Platform, Australia: An integrated intracontinental basin analysis, *Tectonophysics*, 300, 329-358,
929 [https://doi.org/10.1016/S0040-1951\(98\)00253-4](https://doi.org/10.1016/S0040-1951(98)00253-4), 1998.

930 Scott, D. L., Rawlings, D. J., Page, R. W., Tarlowski, C. Z., Idnurm, M., Jackson, M. J., and Southgate, P. N.:
931 Basement framework and geodynamic evolution of the Palaeoproterozoic superbases of north-central Australia:
932 An integrated review of geochemical, geochronological and geophysical data, *Australian Journal of Earth Sciences*,
933 47, 341 - 380, 2000.

934 Southgate, P. N., Bradshaw, B. E., Domagala, J., Jackson, M. J., Idnurm, M., Krassay, A. A., Page, R. W., Sami, T. T.,
935 Scott, D. L., Lindsay, J. F., McConachie, B. A., and Tarlowski, C.: Chronostratigraphic basin framework for

936 Palaeoproterozoic rocks (1730-1575 Ma) in northern Australia and implications for base-metal mineralisation,
 937 Australian Journal of Earth Sciences, 47, 461 - 483, 2000a.

938 Southgate, P. N., Scott, D. L., Sami, T. T., Domagala, J., Jackson, M. J., James, N. P., and Kyser, T. K.: Basin shape
 939 and sediment architecture in the Gun Supersequence: A strike-slip model for Pb-Zn-Ag ore genesis at Mt Isa,
 940 Australian Journal of Earth Sciences, 47, 509 - 531, 2000b.

941 Southgate, P. N., Kyser, T. K., Scott, D. L., Large, R. R., Golding, S. D., and Polito, P. A.: A basin system and fluid-
 942 flow analysis of the Zn-Pb-Ag Mount Isa-type deposits of northern Australia: Identifying metal source, basinal
 943 brine reservoirs, times of fluid expulsion, and organic matter reactions, Economic Geology, 101, 1103-1115,
 944 10.2113/gsecongeo.101.6.1103, 2006.

945 Southgate, P. N., Neumann, N. L., and Gibson, G. M.: Depositional systems in the Mt Isa inlier from 1800 Ma to
 946 1640 Ma: Implications for Zn-Pb-Ag mineralisation, Australian Journal of Earth Sciences, 60, 157-173, 2013.

947 Sweet, I. P.: Carrara Range region NT Geological Map Commentary. Record 6460. , Geoscience Australia,
 948 Canberra, 1984.

949 Sweet, I. P.: The geology of the South Nicholson Group, northwest Queensland. Queensland Geological Record
 950 2017/07, 2017.

951 Thomas, D. W., and Coward, M. P.: Late Jurassic-early Cretaceous inversion of the northern east Shetland Basin,
 952 northern North Sea, Geological Society, London, Special Publications, 88, 275-306, 10.1144/gsl.sp.1995.088.01.16,
 953 1995.

954 Turner, J. P., and Williams, G. A.: Sedimentary basin inversion and intra-plate shortening, Earth-Science Reviews,
 955 65, 277-304, <https://doi.org/10.1016/j.earscirev.2003.10.002>, 2004.

956 Withnall, I. W.: Geochemistry and tectonic significance of Proterozoic mafic rocks from the Georgetown Inlier,
 957 north Queensland, BMR Journal of Australian Geology & Geophysics, 9, 339-351, 1985.

958 Withnall, I. W., and Hutton, L. J.: Chapter 2: North Australian craton, in: Geology of Queensland, edited by: Jell, P.
 959 A., Geological Survey of Queensland, Brisbane, 23-112, 2013.

960 Yang, B., Collins, A. S., Cox, G. M., Jarrett, A. J. M., Denyszyn, S., Blades, M. L., Farkaš, J., and Glorie, S.: Using
 961 Mesoproterozoic sedimentary geochemistry to reconstruct basin tectonic geography and link organic carbon
 962 productivity to nutrient flux from a northern Australian large igneous province, Basin Research, n/a,
 963 10.1111/bre.12450, 2020.

964 Yang, J., and Radulescu, M.: Paleo-fluid flow and heat transport at 1575 Ma over an E-W section in the northern
 965 Lawn Hill Platform, Australia: Theoretical results from finite element modeling, Journal of Geochemical
 966 Exploration, 89, 445-449, <https://doi.org/10.1016/j.gexplo.2005.11.079>, 2006.

967

968 **Figure Captions**

969 Figure 1. (a) Simplified geological map for northern Australia showing principal tectono-morphological
 970 elements and Pb-Zn mineral deposits (after Jackson et al., 2000). (b) More detailed geological map of
 971 periclinal folds developed in inverted stratigraphy of the Isa Superbasin on the Lawn Hill Platform east of
 972 Century Mine and seismic reflection lines 06GA-M1 and 06GA-M2 along which these structures are
 973 imaged. Figure reproduced with permission under the Creative Commons Attribution 4.0 International
 974 Licence: <http://creativecommons.org/licenses/by/4.0/legalcode>. © Commonwealth of Australia
 975 (Geoscience Australia) 2020.

976 Figure 2. Map showing presently defined limits of outcropping Leichhardt, Calvert and Isa superbasins
 977 across the Mount Isa region. Seismic reflection data indicate that all three basins are variably preserved in
 978 the subsurface geology beneath the South Nicholson and Georgina basins and continue northwards into the
 979 McArthur Basin and Batten Trough (see Carr et al., 2019). Reproduced with permission: Licensed CC BY
 980 version 4.0 © State of Queensland, 2020.

981 Figure 3. Simplified stratigraphic column for Mount Isa region and neighbouring southern McArthur
 982 Basin showing three-fold subdivision into Leichhardt, Calvert and Isa superbasins but different
 983 interpretations of basin history and tectonic evolution (Betts and Lister, 2001; Betts et al., 2003; Gibson et

984 al., 2016;Southgate et al., 2000a). The Carrara Range Group is shown as part of the lower Tawallah
985 Group and a correlative of the Leichhardt Superbasin based on revised mapping (Rawlings et al., 2008)
986 and recently published geochronological data (Kositcin and Carson, 2019) for the McArthur Basin.
987 Vertical blue lines represent periods of non-deposition or missing geological record; open circles = basal
988 conglomerates; vvv = basaltic volcanic rocks. Individual Pb–Zn deposits are shown as yellow stars: 1=
989 Mount Isa; 2=Lady Loretta; 3=McArthur River; 4=Century.

990 Figure 4. South Nicholson seismic grid and late Paleoproterozoic–early Mesoproterozoic basinal sequences
991 draped over gravity image for region west of Lawn Hill Platform. Note anomalously deep gravity low
992 centred on the Carrara Sub-basin (Carr et al., 2019) which is bounded by the Carrara Range (gravity high)
993 to the north of line 17GA–SN1. Geology modified from Rawlings et al. (2008) and Ahmad & Munson
994 (2013). Gravity image reproduced with permission under the Creative Commons Attribution 4.0
995 International Licence: <http://creativecommons.org/licenses/by/4.0/legalcode>. © Commonwealth of
996 Australia (Geoscience Australia) 2020.

997 Figure 5. Basin and basement architecture for northern Lawn Hill Platform showing main depocentres,
998 fault trends and depth to magnetic basement for Isa Superbasin (after Gorton and Troup, 2018 from image
999 created by Frogtech Geoscience, 2018). Seismic lines are shown in various colours and include the 1994
1000 (Comalco) and 2011 (Teck Resources) industry surveys across the Isa Superbasin and adjacent Punjaub
1001 Structure (P). Yellow lines are for composite image presented in Figures 6–7. Note compartmentalisation
1002 of depocentres brought about by interference between the ENE and NW-trending faults; latter are of
1003 Calvert age and include older normal faults (e.g. Riversleigh Fault) reactivated as strike-slip structures
1004 during crustal extension accompanying formation of the Isa Superbasin. Figure is reproduced with
1005 permission under the Creative Commons Attribution 4.0 International Licence:
1006 <http://creativecommons.org/licenses/by/4.0/legalcode>. © State Government of Queensland (Geological
1007 Survey of Queensland, Georesources Division, Department of Natural Resources, Mines and Energy)
1008 2020.

1009 Figure 6. North-south oriented transect across northern Lawn Hill Platform made up of selected industry
1010 and government seismic sections (Fig. 5) showing predominance of north-dipping normal faults on which
1011 there has been successive episodes of basin inversion, leaving behind a legacy of fault reactivation and
1012 periclinal folding in (a) Punjaub Structure and (b) Mount Caroline and Ploughed Mountain (after Gibson et
1013 al., 2017; 2020). Note thinning of River and Term supersequences northward through onlap in (a); the
1014 underlying Loretta Supersequence similarly thins northward but is bounded top and bottom by truncated
1015 surfaces thought to reflect considerable loss of stratigraphic section by uplift and erosion accompanying the
1016 1650–1640 Ma Riversleigh Tectonic Event. Sedimentary patterns point to growth faulting on north-dipping
1017 structures during deposition of the Isa, but not underlying Calvert Superbasin whose sequences are merely
1018 offset. Bluewater, Boga and Tin Tank Fault names adopted from Bradshaw et al (2018) and unpublished
1019 industry maps (Minerals, 2017). In (b) the older sequence had already been folded before the River
1020 Supersequence was deposited as evidenced by thinning of the latter over the crests of folds developed in
1021 the Calvert Superbasin at deeper levels beneath Mount Caroline. The Calvert Superbasin is in turn separated
1022 by an angular unconformity from an even older underlying sequence inferred (Gibson et al., 2017;Gibson
1023 et al., 2016) to be the Leichhardt Superbasin. Colour coding is same as Figure 3.

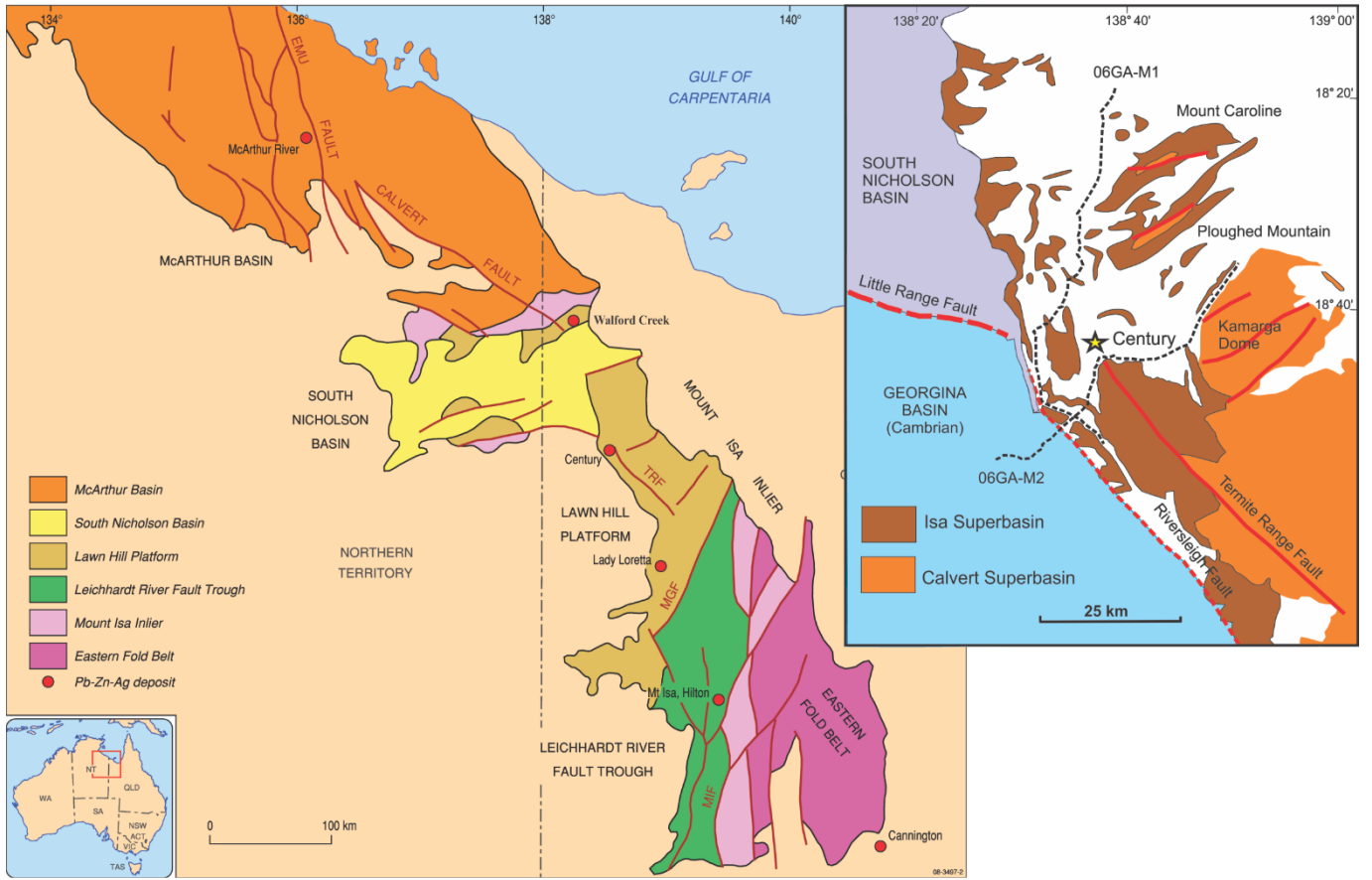
1024 Figure 7. West-east oriented seismic transects through northern Lawn Hill Platform. Westward thickening
1025 of Calvert-age sedimentary units in both (a) and (b) is consistent with growth faulting on east-dipping
1026 normal faults which have since been variably reactivated (Isa Orogeny). Conversely, no such growth is
1027 obviously developed in the overlying Isa Superbasin whose lithological strike and inversion structures are
1028 essentially parallel to the line of section. These units still thicken into the centre of the Isa Superbasin but

1029 in a direction orthogonal to normal faults active during its deposition. Such faults, if imaged, would be
1030 expected to be flat-lying or have very shallow dips parallel or subparallel to bedding in both sections rendering
1031 their recognition very difficult. Some of the disruption to bedding in (b) along line 90Bn10 may be due to
1032 such faults but overall the most obvious structural feature in the section is the broad arching and folding of
1033 stratigraphy in the middle of the section consistent with imaging of an inversion fold in longitudinal cross-
1034 section. Note truncated surface and angular unconformity at base of Loretta in both sections which is
1035 interpreted here to be an expression of basin inversion linked to the 1650-1640 Ma Riversleigh Tectonic
1036 Event.

1037 Figure 8. West-east oriented section through (a) Century Mine (06GA-M2); (b) its western continuation
1038 (17GA-SN1) across the South Nicholson Basin and Carrara Sub-basin (Carr et al., 2019); and (c) enlarged
1039 section of 17GA-SN1 showing angular unconformity between Isa Superbasin and an underlying, variably
1040 truncated older basin sequence. This older basin sequence directly overlies crystalline basement and likely
1041 comprises rocks of the Leichhardt Superbasin, correlatives of which (Carrara Range Group) are exposed in
1042 the Carrara Range immediately to the north of seismic line 17GA-SN1 (see Fig. 4). Note also that this older
1043 sequence is contiguous with rocks in the Century region (06GA-M2) previously identified as part of the
1044 Leichhardt Superbasin (Gibson et al., 2017). Conversely, the Calvert Superbasin is missing west of the
1045 Riversleigh Fault consistent with non-deposition or a period of uplift and erosion during the course of which
1046 it and a significant amount of the underlying Leichhardt Superbasin were removed from the geological
1047 record.

1048 Figure 9. North-south oriented seismic sections west of Lawn Hill Platform showing shallow crystalline
1049 basement and same basement-rooted inversion structure. Note major basement structure in (a) that cuts
1050 downward all the way to the MOHO is probably the same basement structure imaged in (b) and over which
1051 all older sedimentary basins have been eroded so that rocks of Cambrian age (Georgina Basin) directly
1052 overlie basement (17GA-SN4). Rocks of the South Nicholson have similarly been removed for the crest of
1053 this basement block in 17GA-SN4 and, together with rocks of the Isa Superbasin, increase in thickness
1054 northwards. The Isa Superbasin is abruptly truncated by the basement structures and other subvertical
1055 structures suggestive of a flower structure and late-stage onset of strike-slip faulting at or before deposition
1056 of Cambrian Georgina Basin.

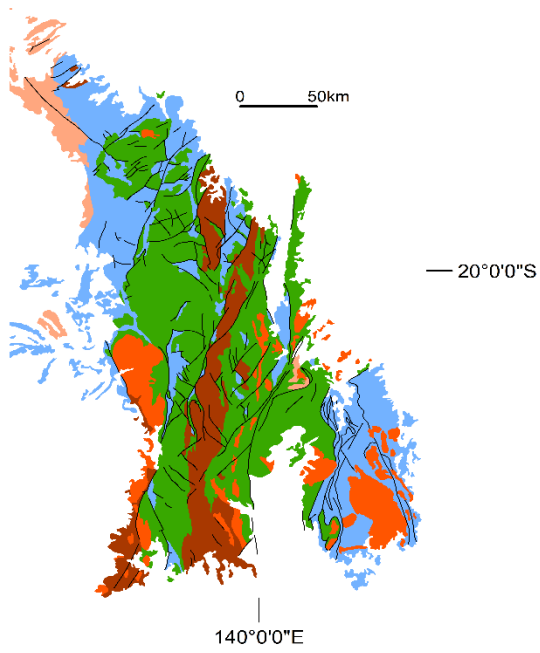
1057 Figure 10. Basin inversion and resulting styles of structural architecture to be anticipated during crustal
1058 shortening (after Martinez et al, 2012; McClay, 1995): (a) early normal fault; (b) harpoon structure from
1059 partially inverted normal fault; (c) buttressing; (d) hangingwall is faulted forming hangingwall shortcut; (e)
1060 footwall shortcut thrust; (f) folding and truncation of normal fault by younger thrust; (g) thrust ramp above
1061 normal fault.



1062

1063

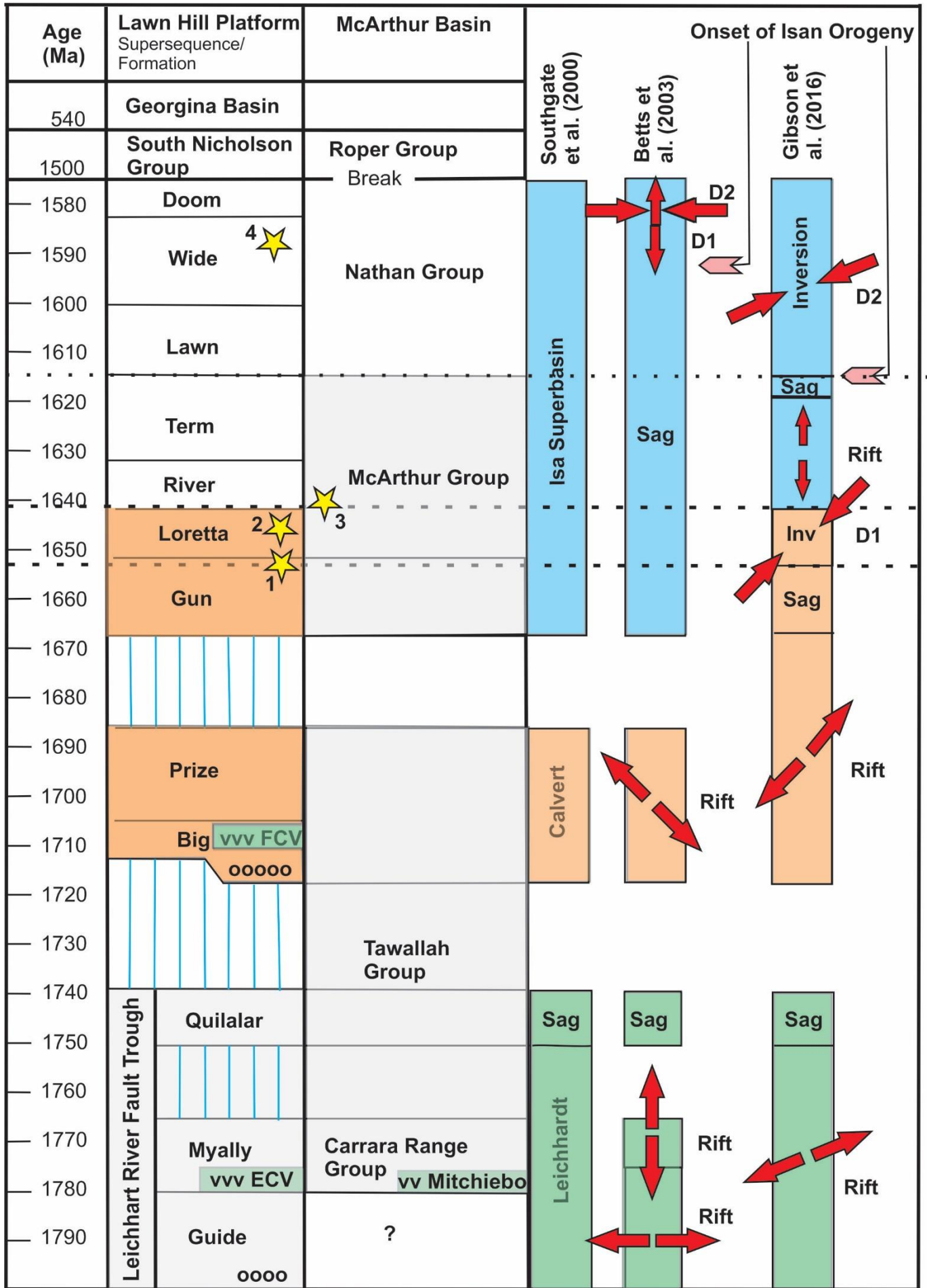
Figure 1



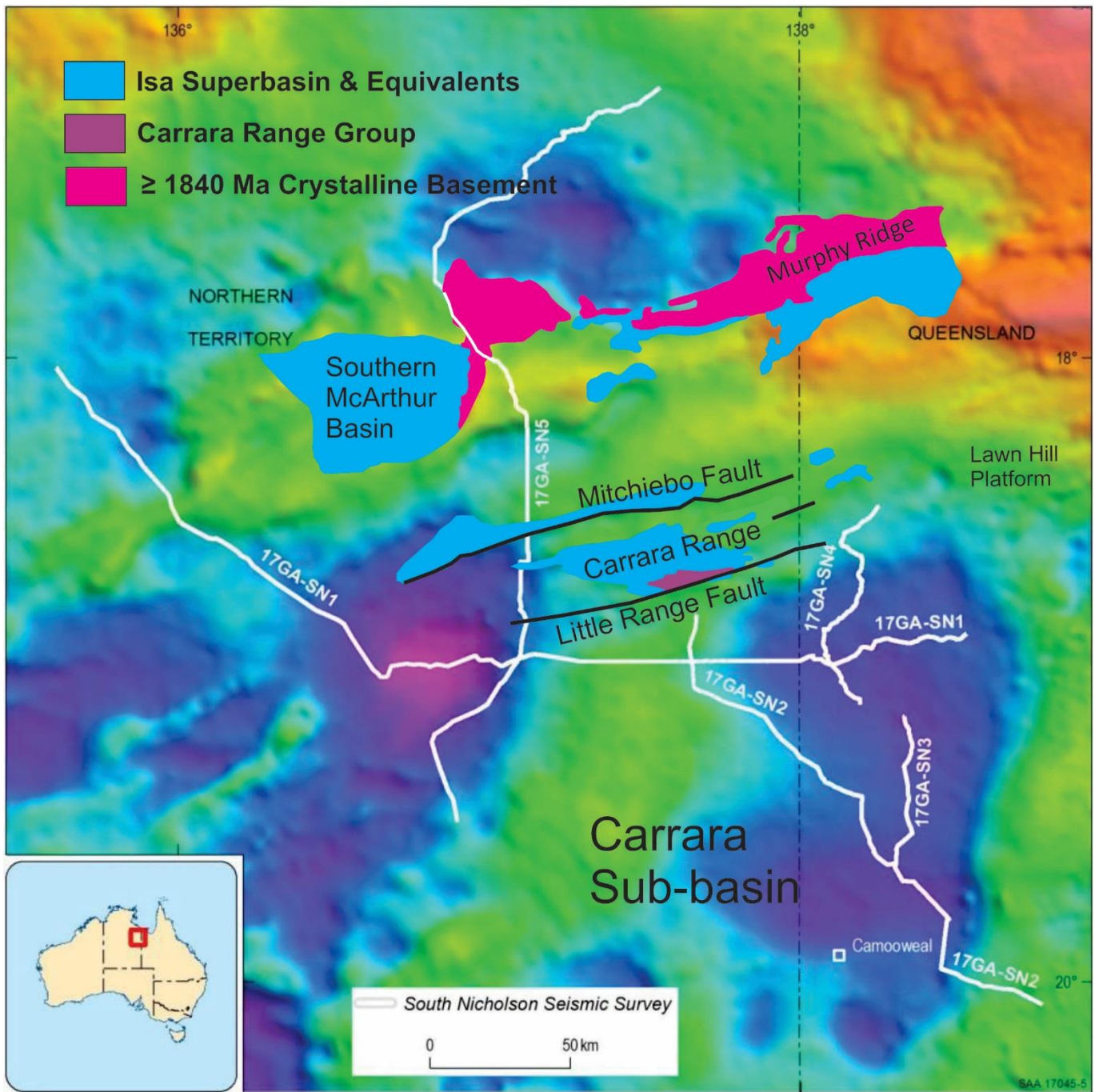
- Plutonic Suites
- Isa Superbasin
- Calvert Superbasin
- Leichhardt Superbasin
- pre-Leichhardt basement

1064

1065 Figure 2

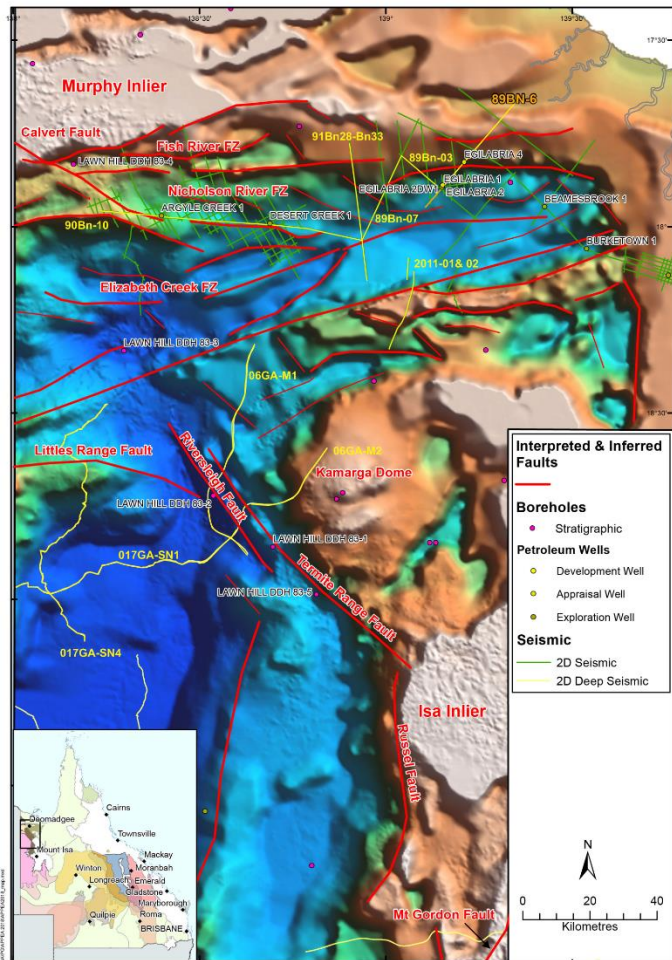


1067 Figure 3



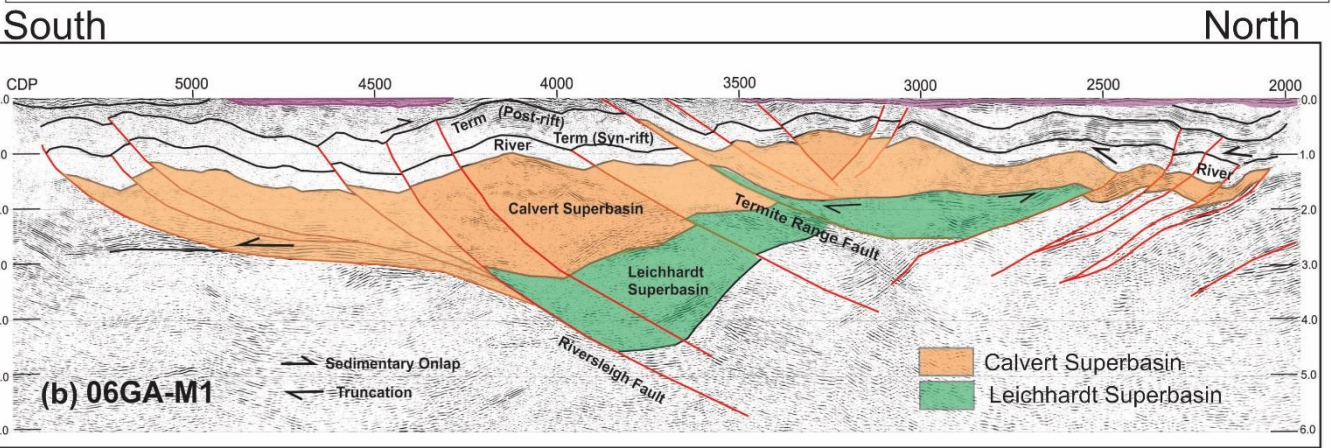
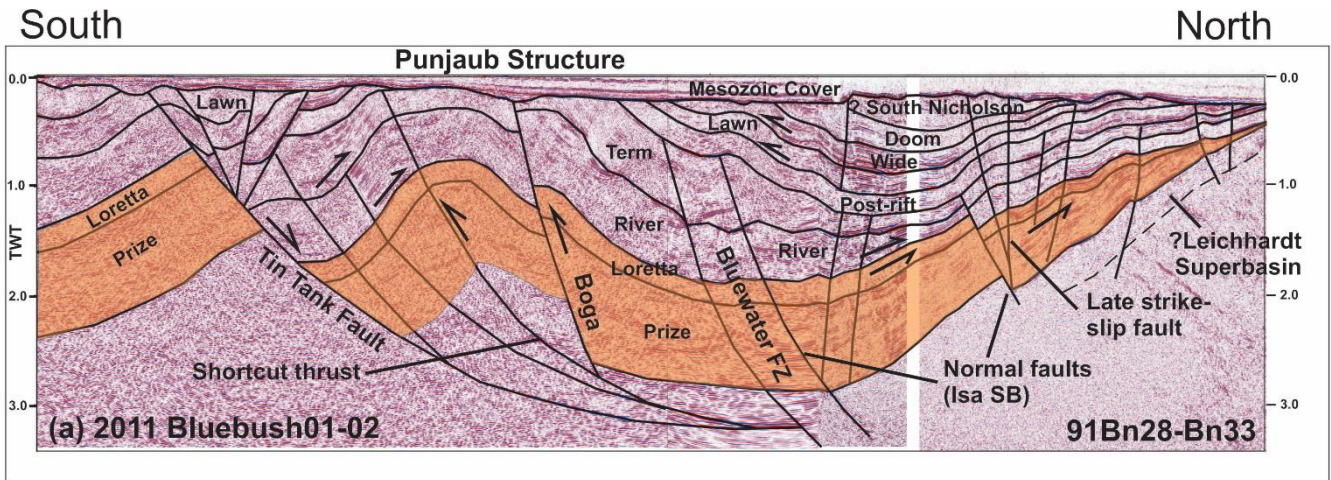
1068

1069 Figure 4



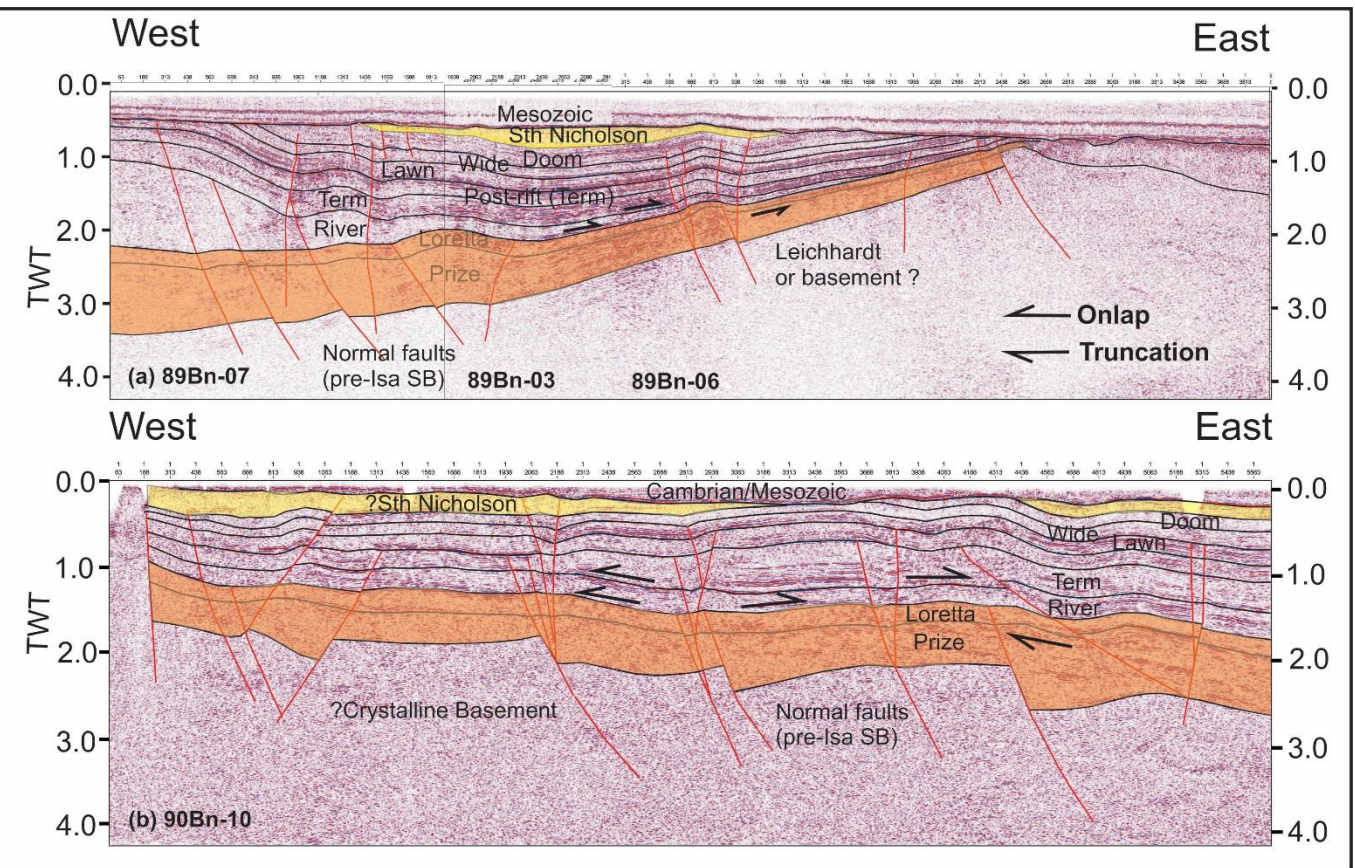
1070

1071 Figure 5



1072
1073

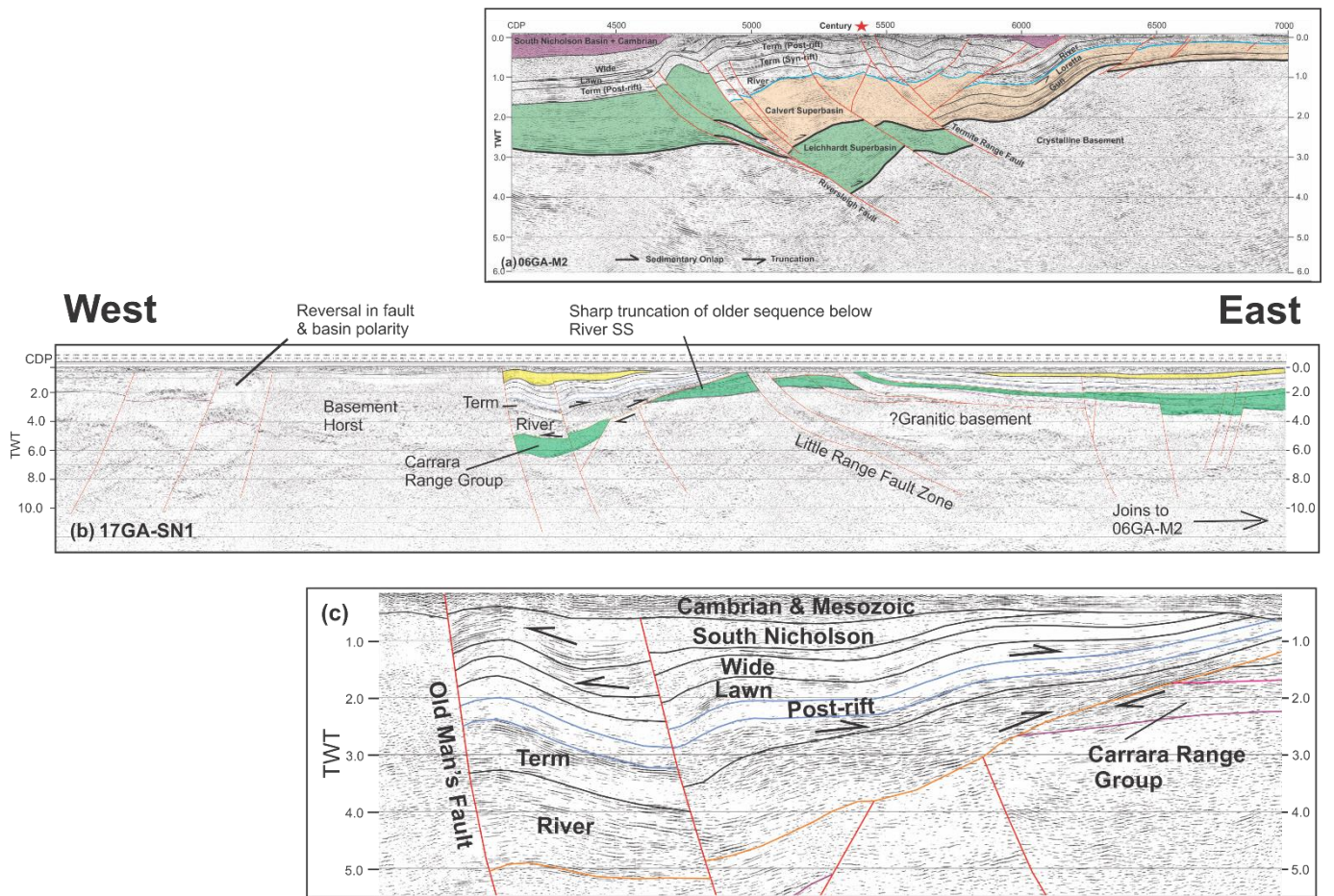
Figure 6



1074

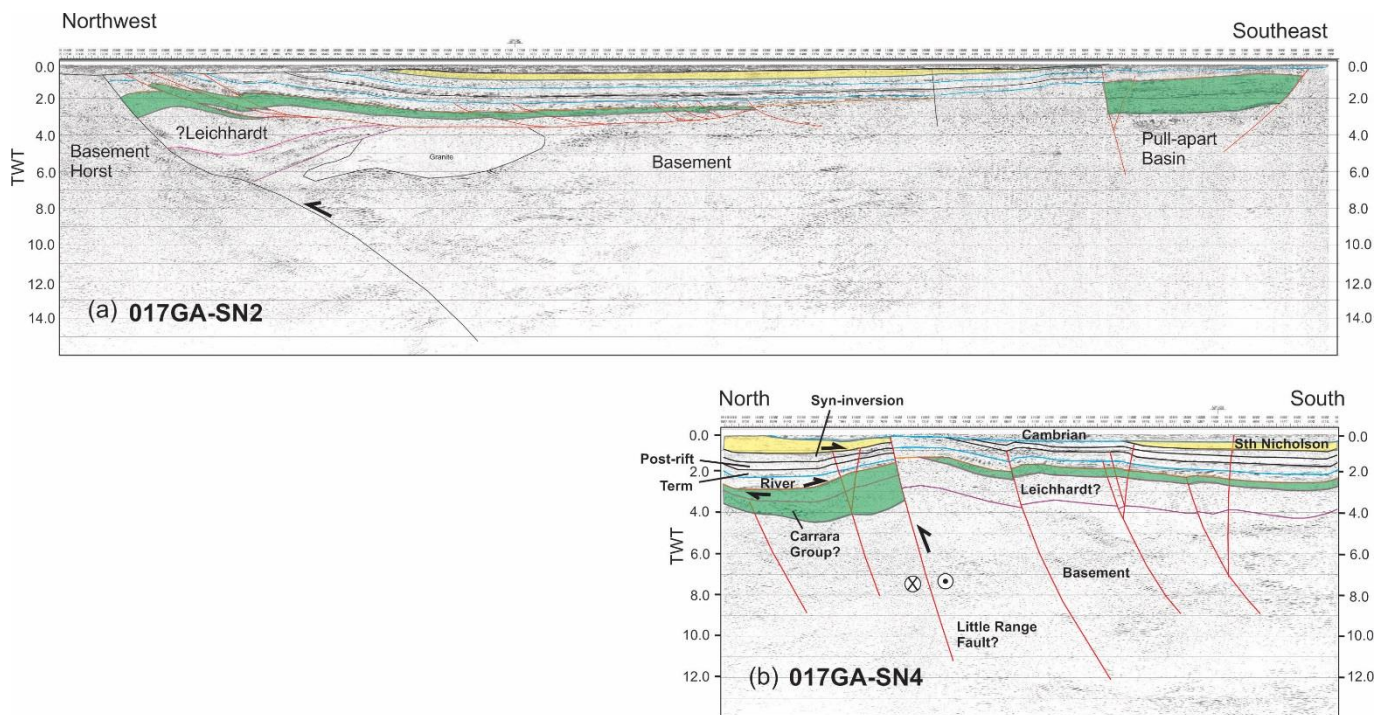
1075 Figure 7

1076



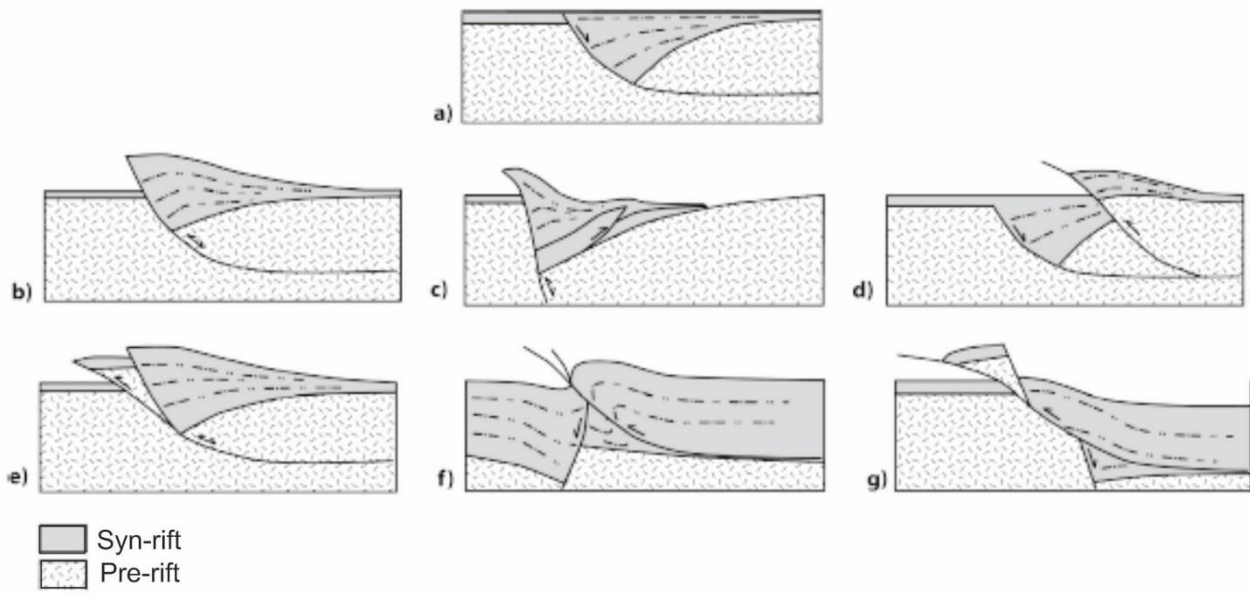
1077

1078 Figure 8



1079

1080 Figure 9



1081

1082 Figure 10